Ecological Informatics 78 (2023) 102352

Contents lists available at ScienceDirect

Ecological Informatics

journal homepage: www.elsevier.com/locate/ecolinf

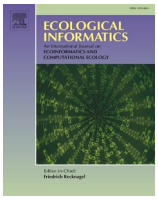

Comparing the ability of different remotely sensed evapotranspiration products in enhancing hydrological model performance and reducing prediction uncertainty

Soufiane Taia [a], Andrea Scozzari [b,*], Lamia Erraioui [a], Malika Kili [a], Abdelaziz Mridekh [a], Souad Haida [a], Jamal Chao [a], Bouabid El Mansouri [a]

[a] Natural Resources and Sustainable Development Laboratory, Ibn Tofail University, Campus Maamora, 14000 Kenitra, Morocco
[b] Institute of Information Science and Technologies (CNR-ISTI), National Research Council of Italy, 56124 Pisa, Italy

ARTICLE INFO

Keywords:
SWAT model
Sufi2
Calibration
Uncertainty
Actual evapotranspiration
Global datasets
High atlas

ABSTRACT

The mitigation of uncertainties in the identification of natural systems is a fundamental aspect in the development of hydrological models, and represents a major challenge for the improvement of modelling techniques. In particular, the calibration of hydrological models based on streamflow measurements at the outlet of a catchment is exposed to significant sources of uncertainty, such as the impact of landscape features on runoff generation. Remote sensing-based actual evapotranspiration (AET) data can be incorporated with streamflow to improve model accuracy and reduce the uncertainty in hydrological modelling, resulting in a significant enhancement of the model performance. The selection of the right AET dataset for hydrological modelling is a crucial task, in front of the availability of multi-source datasets that differ in methods, parameters, and spatiotemporal resolution. Despite the existence of a few studies proposing the usage of remote sensing-based AET data, there is a lack of systematic comparisons between different products, in terms of performance for hydrological modelling. This paper aims to compare the efficacy of different remote sensing-based AET products in improving the simulation of hydrological responses, both in single and in multi-variable scenarios. In this investigation, the Soil and Water Assessment Tool (SWAT) hydrological model was calibrated with observed streamflow data by experimenting with eight different AET datasets. The findings of our study suggest that the incorporation of remote sensing-based AET data in the calibration process of a hydrological model can significantly enhance the accuracy and reliability of model predictions. Thus, the proposed approach can contribute to improving the effectiveness of hydrological modelling as a quantitative tool for the management of water resources. Another finding of this study is that the calibration of the model based solely on AET yields reasonable simulation results of the streamflow, which is an advantageous and promising feature for ungauged basins.

1. Introduction

Hydrological modelling and predictions are playing a key role in the current scenario of climate change, and have an increasing impact on management decisions, planning and resilience to future possible scenarios. Advancements in hydrological modelling techniques are frequently focused on the mitigation of measurement uncertainties and on the reduction of the ambiguities due to the contribution of multiple parameters to the state of a hydrological process. Remote sensing techniques are significantly contributing to the field of hydrological modelling, carrying new possibilities to collect and assimilate data into hydrological models and improve their accuracy.

In particular, physically-based semi-distributed hydrological models involve a high number of parameters to reflect the landscape characteristics (Devia et al., 2015), most of which cannot be directly measured and must be estimated during the calibration process (Abbaspour et al., 2017). Distributed hydrological models are often calibrated using the observed streamflow at the outlet of a catchment (Gupta and Govindaraju, 2022). However, this approach may mislead landscape features that significantly affect runoff generation, because the streamflow embeds contributions from several hydrological components in natural catchments (He et al., 2021; Taia et al., 2023). Moreover, relying simply

* Corresponding author.
E-mail address: a.scozzari@isti.cnr.it (A. Scozzari).

https://doi.org/10.1016/j.ecoinf.2023.102352
Received 28 March 2023; Received in revised form 21 October 2023; Accepted 22 October 2023
Available online 2 November 2023

on a single point for calibrating distributed models may not provide correct simulations in every part of the study area (Sirisena et al., 2020). Thus, the calibration process can be effective for certain parameters and not for others (Abbaspour et al., 2007), and some combinations of parameters may lead to similar objective functions, resulting in ambiguities for the determination of correct values of such parameters (Beven and Freer, 2001). This issue is referred to as "equifinality" in the literature (Beven, 2006). Equifinality increases the uncertainty of parameters, thereby reducing confidence in model predictions (Casado-Rodríguez and del Jesus, 2022; Her and Seong, 2018; Moges et al., 2021). Typical approaches for the mitigation of equifinality can be based on the inclusion of other variables in addition to streamflow measurements, or the usage of non-quantitative data based on experts' knowledge (Efstratiadis and Koutsoyiannis, 2010; Lee et al., 2022; Liu et al., 2020; Tobin and Bennett, 2020).

The calibration of multiple variables can be challenging in data-scarce areas, characterized by insufficient ground measurements. Earth observation datasets based on remote sensing techniques offer an effective solution to this problem (Jeyalakshmi et al., 2021; Nourani et al., 2021; Sun et al., 2019). Remote sensing permits a kind of regular sampling (in time and space) of essential hydrological parameters, such as precipitation, snow cover area, soil moisture, water storage, and evapotranspiration (Chen and Wang, 2018; Shawky et al., 2023; Ustin and Middleton, 2021). By collecting data on relatively large areas at frequent time intervals, remote sensing can help to minimize uncertainties of model parameters that are crucial for an accurate simulation of the water balance (Kunnath-Poovakka et al., 2021; Wambura et al., 2018). Furthermore, remotely sensed data can be used jointly with hydrological models to forecast other variables, such as streamflow, in poorly gauged or even totally ungauged areas (Gleason and Durand, 2020; Jiang and Wang, 2019).

Actual evapotranspiration (AET) is a significant component of the water balance (Zhang et al., 2016), as it transfers soil moisture to the atmosphere, playing a crucial role in the energy and water cycles (Schlesinger and Jasechko, 2014). Consequently, the accurate prediction of AET is important for improving the performance of hydrological models (Jiang et al., 2020; Ukkola and Prentice, 2013). There's an ample literature showing that remotely sensed AET, when incorporated in hydrological modelling, enhances the accuracy and reduces the uncertainty of the model predictions. In particular, several studies demonstrated that MOD16A2 AET data obtained from the Moderate Resolution Imaging Spectroradiometer (MODIS) can enhance hydrological modelling by reducing the degree of equifinality and predictive uncertainties (Koltsida and Kallioras, 2022; Rajib et al., 2018, 2020; Rane and Jayaraj, 2022; Shah et al., 2021; Wambura et al., 2018). Similarly, the AET data from the Global Land Evaporation Amsterdam Model (GLEAM) were found to improve model calibration, permitting accurate simulations of streamflow (Jin and Jin, 2020; López López et al., 2017; Odusanya et al., 2019, 2021; Sirisena et al., 2020).

There are various global AET datasets available, which are essentially based on remotely sensed data, on land surface models, and on hydrological models. These datasets vary in their algorithms, approaches, and also in the spatial and temporal resolutions (Aryalekshmi et al., 2021). Therefore, the selection of the most appropriate AET product to suit a specific study area is crucial. Recent studies, such as those by Chen et al. (2022), Guo et al. (2022a), and Salazar-Martínez et al. (2022), focused on comparing satellite-based AET products with the widely accepted and highly accurate Eddy-Covariance technique to assess their performance in estimating AET across various landscapes and climates. It is also essential to investigate the comparison between AET products in terms of direct effects on the hydrological modelling, in order to understand the impact of their uncertainties on hydrological processes. Studies such as those by Ding and Zhu (2022), and Herman et al. (2018) highlighted that in a given area different AET products can perform differently in terms of parameter calibration for the hydrological simulation. This is due to the differences in AET estimation models and in their input data, which characterise each AET product.

Most of the previous studies using AET for the calibration of hydrological models were limited to the experimentation of only one or two products. Only a limited number of investigations really delved into the performance of various datasets when incorporated in hydrological models. Dembélé et al. (2020) evaluated 12 actual evaporation datasets for their ability to improve the performance of the fully distributed mesoscale Hydrologic Model (mHM). Four distinct multivariate calibration strategies were implemented, based on actual evaporation and streamflow, resulting in 48 scenarios whose results were compared with a benchmark model calibrated solely with streamflow data. Furthermore, Herman et al. (2020) attempted to combine streamflow with 8 distinct remote-sensing AET products in calibrating Soil and Water Assessment Tool (SWAT) parameters. They employed the Non-dominated Sorting Genetic Algorithm III (U-NSGA-III) to compare the different Pareto-optimal solutions resulting from the incorporation of different AET datasets using a multi-variable approach. In addition, Guo et al. (2022b) examined the suitability of five remote-sensing-based AET datasets for calibrating the parameters of the variable infiltration capacity (VIC) hydrological model, with the objective to simulate streamflow and soil moisture.

Our study aims to address several research gaps in the field of incorporating remotely sensed AET in hydrological modelling. Firstly, previous studies have not considered the comparison between several AET products in a single-variable calibration, despite its crucial role in hydrological modelling and potential benefits for predicting streamflow in ungauged basins. An accurate prediction of streamflow in ungauged basins is essential for various ecological applications such as flood forecasting, drought monitoring, and irrigation planning, particularly in countries with limited streamflow data, and where the deployment of new monitoring stations is not yet sufficient. Secondly, we emphasize the importance of considering the impact of additional data on the distribution of the involved parameters and on uncertainty in the model output. While the aforementioned studies focused on optimizing hydrological model parameters to achieve the best fit to observed data, our study recognizes that hydrological models are complex and often rely on numerous input parameters, leading to uncertainty in model predictions. Neglecting to account for parameter uncertainty can lead to inaccurate results and potentially harmful decisions in water resource management and hydrological forecasting (Abbaspour et al., 2017). Thirdly, our study investigates the potential benefits of using remote-sensing-based AET products in hydrological modelling over regions in the Atlantic, particularly in Morocco, where the current literature is lacking. This investigation has the potential to provide valuable information to the stakeholders, enabling them to gain insights into the available AET products and their effectiveness in the region, thereby allowing them to select the appropriate product for a given purpose.

In light of this, we experimented with eight different AET datasets in both single and multi-variable calibration alongside streamflow data and we extended the analytical approach with respect to the former literature, by incorporating the predictive uncertainty derived from parameter distribution with the Sequential Uncertainty Fitting v2 algorithm (Sufi2). The SWAT model was chosen for this study as it has been previously implemented and validated in the same catchment of this study (Taia et al., 2023), making it a suitable tool for further hydrological modelling analyses. Therefore, the current study offers a systematic comparison of the performance of AET datasets and their effectiveness in reducing parameters and predictive uncertainties in a SWAT hydrological model. As detailed in Section 2.1, two sub-catchments of the Oued El Abid catchment in the central High Atlas of Morocco were chosen for this purpose.

The primary objectives of this study are: (1) evaluate the ability of a single-variable approach for calibrating the SWAT model to predict streamflow, by experimenting with eight different remotely sensed AET products; (2) assess the effectiveness of a two-variable calibration approach (combining remotely sensed AET data and streamflow

observations) for improving the model's robustness, its ability to make accurate predictions, and for better quantifying model parameters.

2. Materials and methods

To address the objectives of this study, we implemented the SWAT model for the Oued El Abid catchment, as detailed in the next section. This task entailed the assimilation of data about land use, soil attributes, elevation, and climatic conditions. Then, model calibration was done by using both AET and streamflow through distinct scenarios. In some scenarios, the calibration was exclusively based on AET, providing insights into the impact of using this variable alone. In contrast, other scenarios combined both AET and streamflow, enabling an assessment of a multi-calibration strategy.

The Sufi2 algorithm facilitated the optimization of relevant parameters of the SWAT model for each scenario. Addressing questions of performance and uncertainty demanded a comprehensive analysis of the uncertainty for both output and parameters, along with an assessment of equifinality. We employed methods like the posterior distribution for analysing parameters' uncertainty and leveraged the 95% prediction uncertainty concept to estimate the predictive uncertainty originated by variations of the parameters.

2.1. Study area

This research has been carried out on the 7950 km^2 Oued El Abid catchment, which is a major sub-catchment of the Oum Er-Rbia basin, located in the central High Atlas of Morocco. The catchment of Oued El Abid is characterized by extremely high evaporation rate, where snowfall plays a primary role in its water cycle, as reported by Taia et al. (2023), and Tuel et al. (2021). The Oued El Abid river feeds one of Morocco's main dams, the Bine El Ouidane dam. In addition to supplying irrigation and drinking water to the population of the central High Atlas, this dam is also vital for hydropower generation, making the economy of the region very vulnerable to water scarcity. Nevertheless, significant climatic changes, including frequent droughts and rising precipitation variability, have been reported in this region (El Khalki et al., 2021). Thus, new modelling approaches are of great importance for a better planning and for an improved allocation of water resources in the area.

The main river in the region of Oued El Abid originates from the northeast and flows towards the west, converging with the Ahmed Ahansal river that drains water from the southern region. Together, these rivers provide an annual volume of freshwater to the Bine El Ouidane dam ranging from 400 to 1500 Mm^3. The elevation of the Oued El Abid catchment varies from 3690 m at Jbel Azourki in the east to 300 m in the plain downstream of Bine El Ouidane (Fig. 1). Runoffs progressively pass from a regime of rain to snow-rain, then to purely snow depending on the elevation. The land cover in the catchment is mainly composed of bare soil, scrub and forest with some croplands. The annual mean rainfall in the north-eastern part of the catchment is around 450 mm, whereas in the western part, it is <250 mm. Oued El Abid's catchment experiences significant seasonal temperature variations, with winter temperatures as low as −9 °C and summer temperatures reaching 43 °C. Average temperatures range from 15 °C to 18 °C up to 1500 m, decreasing rapidly at higher altitudes.

2.2. Setting up the SWAT model for the Oued El Abid catchment

2.2.1. SWAT model description

SWAT is a hydrological model for the simulation of surface and

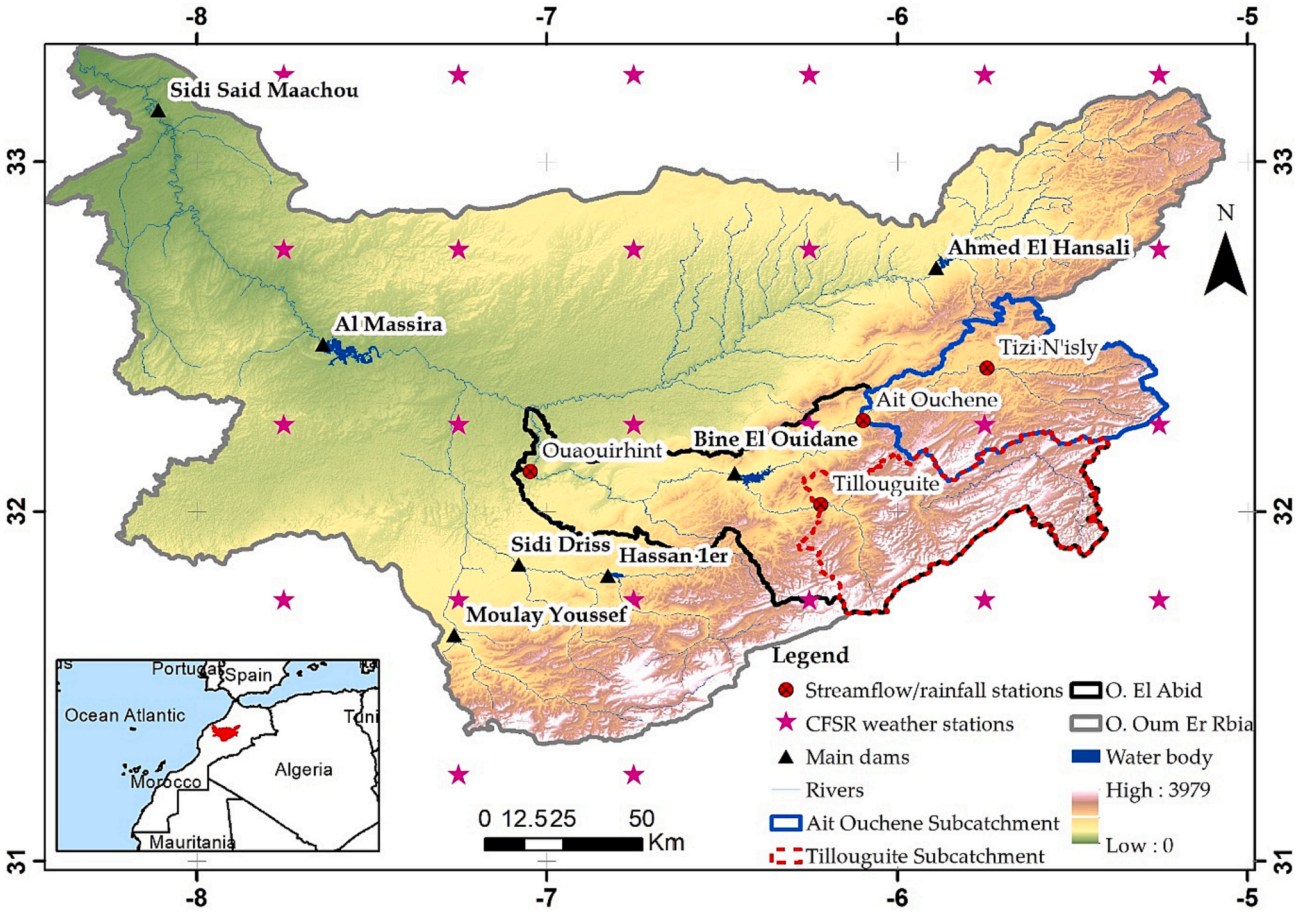

Fig. 1. Location map of the study area depicting elevation, streamflow and rainfall gauges, and main dams.

groundwater quantity and quality, capable to simulate eco-hydrological and anthropogenic processes at various scales, from small catchments to full river basins (Acharki et al., 2023; Erraioui et al., 2020; Strauch et al., 2012; Taia et al., 2021). As per Neitsch et al. (2011), SWAT hydrological processes are modelled in two distinct stages: the land phase and the routing phase. The land phase determines the presence of water, sediment, nutrients, and pesticides in each subbasin, while the routing phase computes the flow and spread of these elements through the channel network of the catchment. Streamflow in the SWAT model is simulated by considering lateral flow, groundwater flow, and surface runoff. SWAT uses the Soil Conservation Service Curve Number (SCS-CN) method to estimate the surface runoff (Neitsch et al., 2011). Once soil water routing processes are completed (i.e., infiltration, runoff and water intercepted by the plants' canopy), the amount of water required to satisfy evapotranspiration requirements from each soil layer is calculated. Three calculation methods for estimating the potential evapotranspiration (PET) are offered by the SWAT model: Penman-Monteith (Monteith, 1965), Priestley-Taylor (Priestley and Taylor, 1972), and Hargreaves (Hargreaves and Samani, 1985). The Penman-Monteith stands out for its holistic integration of energy and aerodynamics. Its robustness, further endorsed by the Food and Agriculture Organization (FAO), made it our chosen method for this study.

2.2.2. Data used

Table 1 lists the data required for implementing the SWAT model, including elevation, land cover, soil, precipitation, weather, and flow data. The elevation data used were obtained from the Shuttle Radar Topography Mission (SRTM) in a GeoTIFF format, and have a spatial resolution of 30 m. The land cover map was reclassified using a supervised classification based on Sentinel 2 A images and classified into several categories such as farmland, forest, sparse vegetation, water bodies, urban land, and bare land. Soil datasets were extracted using the global soil map of the Food and Agriculture Organization (FAO), spatial soil information from the International Soil Reference and Information Center (ISRIC), and the Harmonized World Soil Database (HWSD). The precipitation datasets used consist in daily data acquired in the period between 1980 and 2015 from 4 ground stations located within and around the catchment area (Fig. 1). The Climate Forecast System Reanalysis (CFSR) provided daily climate data including minimum and maximum temperature, relative humidity, solar radiation, and wind speed. We sourced daily average streamflow data for two stations (Tillouguite and Ait Ouchene) from the Hydraulic Basin Agencies, covering the period 1988–2014. These data originated from continuous water level measurements at hydrometric stations and periodic flow measurements using a v-notch weir. The agencies employed a rating curve to process these measurements, yielding the daily average streamflow values that we adopted. The dataset is predominantly continuous, offering daily streamflow estimates with very few missing samples. The former data were aggregated to monthly values for subsequent use in the calibration process. However, due to gaps in the data, in particular rainfall and streamflow, we employed the Multiple Imputation by Chained Equations (MICE) method to fill in missing values in the dataset (Van Buuren and Groothuis-Oudshoorn, 2011). This method is a sophisticated approach that utilizes a probabilistic model based on the observed data to estimate missing data points. After preparing the data, SWAT model setup was carried out using ArcSWAT 2012 in ArcGIS environment.

Table 1
Input data used to implement the SWAT model.

Data	Resolution	Source
Elevation	Grid cell 30 m	Shuttle Radar Topography Mission (SRTM)
Land use	Grid cell 10 m	Supervised classification of Sentinel 2 A images
Soil	Grid cell 1 km	FAO-UNESCO Global Soil Map and global soil database (HWSD)
Precipitation	Points	Hydraulic basin agency of Oum Er-Rbia (ABHOER)
Weather	Grid cell 38 km	Climate Forecast System Reanalysis (CFSR) database.
Flow	Points	Hydraulic basin agency of Oum Er-Rbia (ABHOER)

Several AET products are available, characterized by different spatial/temporal resolutions and coverages, as well as different algorithms, methods, and approaches. The choice of an AET product depends on the specific goals and constraints of the study, as well as on the availability of the necessary data. In this study, eight freely available AET products have been experimented with, as summarised in Table 2. Fig. 2 shows the monthly and annual trends of AET according to each selected product. The remotely sensed AET products used in this study are the following: GLEAM v3.6a, GLEAM v3.6b, MOD16A2, GLDAS v2.1 (Global Land Data Assimilation System version 2.1), PML v2 (Penman-Monteith-Leuning version 2), TerraClimate, FLDAS (The Famine Early Warning Systems Network Land Data Assimilation System), and SSEBop (Operational Simplified Surface Energy Balance).

We sourced AET datasets in NetCDF and Raster formats, which provided evapotranspiration data at varied spatial resolutions (from 500 m to 27,750 m) and temporal resolutions (daily, 8-day, and monthly). To ensure uniformity in the AET data for the SWAT model calibration, the AET time series for each subbasin were extracted using the weighted average method (Rajib et al., 2018; Zhang et al., 2016). The method involves calculating the area-weighted average AET for each subbasin, by multiplying the AET data for each grid cell within the subbasin by the area of the cell, and then summing the values for all grid cells. This method provides an estimate of the average AET time series for all subbasins. Once the AET time series for each subbasin was extracted, daily and 8-day data were then aggregated to monthly data based on the sum of AET values within each month. After these preprocessing steps, the AET data were ready to be used in the calibration process of the SWAT hydrological model.

2.3. Calibration of the SWAT model

2.3.1. Calibration approach

A set of 17 distinct scenarios was formulated, based on the monthly streamflow data described above and on AET time series from diverse sources.

Reference Scenario (S0): in the initial scenario, the SWAT model was calibrated solely using monthly streamflow measurements taken at the sub-catchment outlet. This method is commonly adopted in modelling literature, especially in data-scarce regions. It serves as a foundational baseline to understand and compare the performance of the model by adding constraints at successive steps

Single-variable AET Scenarios (S1 to S8):eight distinct scenarios were implemented, each of them based on a unique AET dataset from the eight datasets considered for calibrating the SWAT model. The objective was to explore the efficacy of a SWAT model calibrated with AET in predicting streamflow.

Multi-variable Scenarios (M1 to M8): in this set of scenarios we sought to determine if a multi-variable calibration strategy could improve the optimization of the SWAT model. For this purpose, the calibration of the model was done by pairing each of the eight AET datasets with streamflow data at the outlet of the sub-catchment.

For all the scenarios, we adjusted the SWAT model parameters using the SWAT-CUP software. After that, we analysed and compared the outcomes in order to understand how each scenario impacts the calibration process. This comparison gave insights into the best solutions, uncertainties involved, and how parameters change. Moreover, we ran all the mentioned scenarios for two sub-catchments: Tillouguite and Ait Ouchene, simultaneously.

Calibrations of the model were carried out on a monthly basis, covering the period from 2003 to 2014, with the initial five years (1998–2002) used as a warm-up period. The calibrated scenarios were

Table 2
Remotely sensed AET products used in this study.

Products	ET scheme	Temporal resolution	Spatial resolution (m)	Spatial coverage	Temporal coverage	Reference
PML v2	Penman-Monteith-Leuning	8-day	500	Global	2002–2022	(Zhang et al., 2019)
TerraClimate	Soil water balance	Monthly	4638.3	Global	1958–2022	(Abatzoglou et al., 2018)
FLDAS	Land surface model	Monthly	11,132	Global	1982–2022	(McNally et al., 2017)
SSEBop	Penman-Monteith	Monthly	1065.6	Global	2003–2022	(Senay et al., 2013)
GLEAM v3.6a	Priestley-Taylor	Daily	27,750	Global	1980–2022	(Martens et al., 2017)
GLEAM v3.6b	Priestley-Taylor	Daily	27,750	Global	2003–2022	(Martens et al., 2017)
MOD16A2	Penman-Monteith	8-day	500	Global	2000–2022	(Mu et al., 2007, 2011)
GLDAS v2.1	Land Surface Model	3-h	27,750	Global	2000–2022	(Rodell et al., 2004)

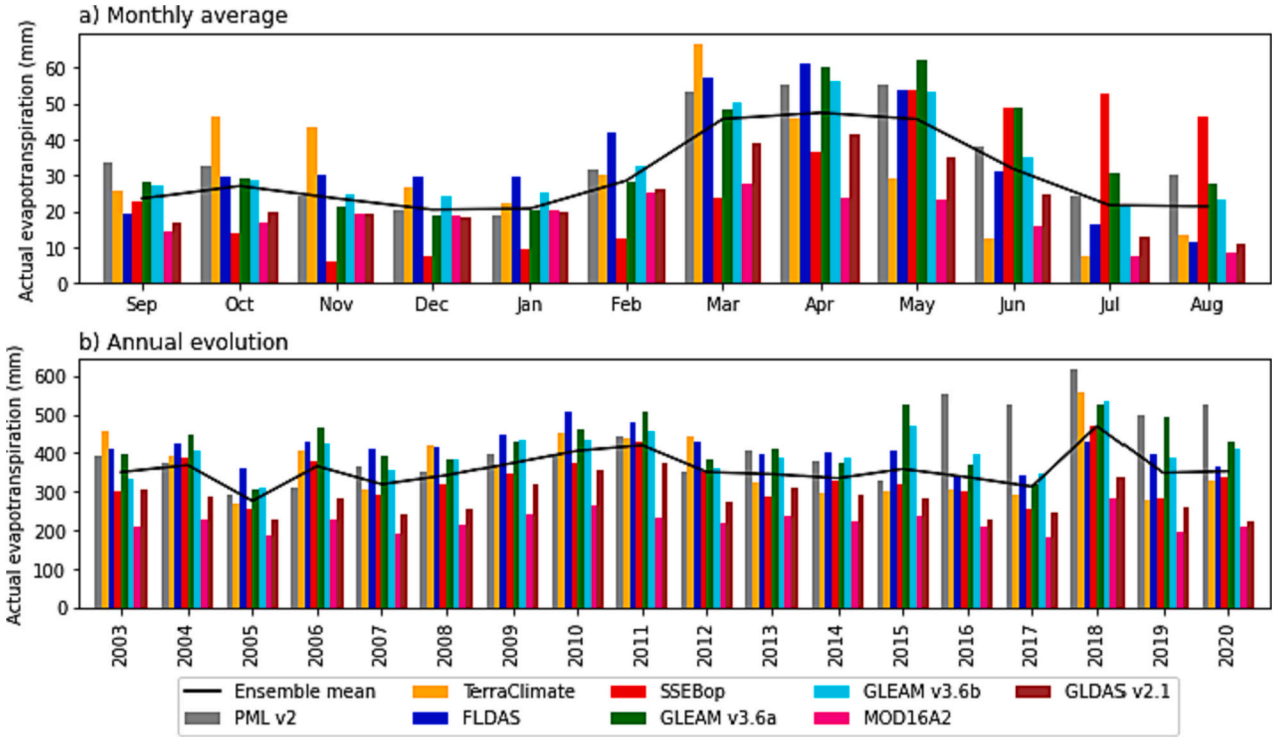

Fig. 2. Monthly average and yearly evolution of AET in the study area.

validated for streamflow during an independent period from 1992 to 2002, with a warm-up period of five years (1988–1992). In our study, we employed an overlapping warm-up period for both calibration and validation phases, specifically from 1998 to 2002. We wish to emphasize that this overlapping period was used exclusively to stabilize the model and did not play a role in the optimization of parameters during calibration. Despite the shared warm-up periods, the data utilized for calibration (2003–2014) and validation (1992–2002) remained distinct and independent, to ensure the integrity and validity of the predictive assessments output by the model.

2.3.2. *Model parameters*

In the study area, snow plays a pivotal role in the water cycle. Thus, the calibration process must prioritize the integration of snow parameters. However, following the guidance of Abbaspour et al. (2015), and Rahman et al. (2013), it's crucial to calibrate snow parameters independently and before other parameters. This initial calibration ensures that the model captures snow processes accurately before delving into the intricacies of other parameters. For our specific objective, which focuses on incorporating remotely sensed evapotranspiration into the calibration process, integrating snow processes may not be appropriate. Thus, the aforementioned parameters were calibrated by strictly using streamflow data. This calibration was later validated with both streamflow and snow cover area data, as outlined by Taia et al. (2023). After determining the optimal values for the snow parameters, they have been fixed before moving on to the other parameters.

The SWAT model manages elevation-related changes by using elevation bands to discretize the snowmelt process based on watershed topography (Grusson et al., 2015). Oued El Abid watershed, known for its steep elevation gradients impacting precipitation and temperature variations. Therefore, we had set five elevation bands (Taia et al., 2023). Two lapse rates (PLAPS) and (TLAPS) are commonly used to adjust precipitation and temperature in the SWAT model according to elevation (Abbaspour et al., 2017). We then included other catchment parameters, incorporating evapotranspiration. This hierarchy was instrumental to examine whether possible alterations of parameters could be directly linked to the integration of evapotranspiration in the calibration process. The selection of the SWAT parameters was based on a rigorous sensitivity analysis. We conducted this analysis using both Q and AET as single and multi-variable criteria across several parameters sets. Parameters that yielded a *p*-value above 0.05 in all scenarios were deemed statistically insignificant and were consequently excluded from the analysis. This approach ensures that the parameters included in the calibration process are relevant and significant to the model.

Establishing the bounds (i.e. the absolute minimum and maximum) of the parameters to be optimized (listed in Table 3) is a fundamental aspect in the preparation of the model. Without any prior information on the distribution of the parameters, we assume that all parameters have

Table 3
Calibrated parameters and their initial ranges. The prefixes v_, and r_ indicate a replacement, and relative change to the initial parameter value.

Parameter	Description	Min	max
v_TLAPS.sub	Temperature lapse rate (°C/km)	−7	2
v_PLAPS.sub	Precipitation lapse rate (mm/km)	0	200
r_CN2.mgt	Curve number	−0.35	0.3
v_ALPHA_BF.gw	Baseflow alpha factor	0	1
r_ESCO.hru	Soil evaporation compensation factor	−0.2	0.2
v_LAT_TIME.hru	Lateral flow travel time (days)	0	20
v_SLSOIL.hru	Slope length for lateral subsurface flow (m)	0	80
v_CANMX.hru	Maximum canopy storage (mm H2O)	0	40
v_CH_N2.rte	Manning's "n" value for the main channel	0.05	0.15
v_CH_K2.rte	Effective hydraulic conductivity in main channel alluvium (mm/h)	0	50
r_SOL_AWC().sol	Available water capacity of the soil (mmH_2O/mmSoil)	−0.1	1
r_SOL_BD().sol	Moist bulk density (Mg/m3)	−0.3	0.3
v_BLAI{8}.plant.dat	Maximum potential leaf area index	0.5	10
v_DLAI{8}.plant.dat	Fraction of growing season when leaf area begins to decline.	0.15	1

an equal distribution within the defined ranges (Abbaspour et al., 2015). Thus, it is critical to determine a reasonable range for each parameter, in order to obtain a well performing calibrated model (Kayastha et al., 2011). This task can be based on existing data about the catchment and on knowledge gained by previous studies. The absolute boundaries of each parameter play a significant role in restricting the solution; former literature shows that a trade-off is necessary for assessing such boundaries, keeping them as large as possible while being physically meaningful (Abbaspour et al., 2007).

In SWAT, the HRU represents the smallest spatial entity within a watershed. Watersheds are divided into elementary items (HRUs) based on factors like elevation, soil, and land use. Given this granularity, spatial parameters such as hydraulic conductivity, bulk density, or CN2 can potentially be defined for each HRU. This detailed categorization poses a challenge for the analysts, as it requires the collection or estimation of numerous input parameters, which are often not readily available. Instead of defining each parameter individually, an alternative strategy is to group or lump them based on attributes like soil type, land use, location, slope, or a mix of them. These lumped parameters can then be calibrated using a global modification term, either multiplicative or additive, thus simplifying the process. Therefore, the v_ prefix indicates a direct replacement of the original value with a new one, while the r_ prefix signifies a modification where the original value is multiplied by (1 + the given r_ value). These prefixes offer a systematic approach to adjust the parameters' values for diverse model simulations.

This process underwent several iterations, each one comprising 600 simulations based on 600 sets of parameters obtained through the Latin Hypercube approach (Abbaspour, 2013). During each iteration, the prior parameter ranges were fine-tuned by calculating the sensitivity matrix (equivalent to the Jacobian), the Hessian matrix, and the covariance matrix, as well as the 95% confidence intervals and correlation matrices of the parameters (Abbaspour et al., 2007). Given the wide range of parameters involved, further rounds of sampling were necessary, involving the refinement of the parameter ranges to make them narrower and focused on achieving optimal simulation (Abbaspour, 2013).

The sensitivity analysis, calibration, and validation were carried out using the SWAT-Calibration and Uncertainty Programs (SWAT-CUP) software (Abbaspour, 2013).

2.3.3. Sensitivity analysis

To assess the relative sensitivity of the selected parameters (see Table 3), 2000 simulations for each sub-catchment (Tillouguite and Ait Ouchene) were carried out. By 'relative sensitivity,' we refer to the degree to which a slight change in a particular parameter influences the model's output, in comparison to changes in other parameters. Essentially, we're evaluating which parameters have the most significant effect on the objective function. The relative sensitivity was computed by using the following multiple regression approach, which regresses the sampled parameters' values against their corresponding objective function values (Abbaspour et al., 2007):

$$g = \propto + \sum_{i=1}^{m} \beta_i b_i.$$

Relative sensitivity was estimated based on linear approximations. A *t-stat* factor was computed to assess the sensitivity. It is the coefficient of a parameter (β_i) divided by its standard error. The *t-stat* measures the precision of the regression coefficient. A parameter is considered "sensitive" when its regression coefficient is relatively larger than its standard error, resulting in a larger absolute *t-stat*. The significance of the sensitivity of each parameter is then calculated by using the *p-value* test. Each parameter's *p-value* tests the null hypothesis, i.e., that the coefficient equals zero (no effect). Thus, the parameter is more sensitive when the t-stat is large and the *p-value* is relatively small, e.g., lower than 0.05 as a practical value.

2.3.4. Performance criteria

Percent Bias (PBIAS) and Nash Sutcliffe Efficiency (NSE) were used to evaluate the SWAT model performance. PBIAS measures the tendency of the model to overestimate or underestimate data values, while NSE assesses its ability to reproduce the observed variability. Both metrics provide a comprehensive evaluation of the model accuracy in simulating hydrological processes (Moriasi et al., 2007).

In multi-variable optimisation, the objective function is defined as:

$$g = \sum_{j} w_j g_j$$

Where w_j is the weight of the $j - th$ variable.

2.4. Uncertainty analysis

The Sufi2 algorithm (Abbaspour, 2013) was employed to perform a predictive uncertainty analysis of the model's output. This implied the adoption of Latin hypercube sampling to propagate the uncertainty of each parameter and calculate the cumulative distribution of each variable at its 2.5% and 97.5% levels. In fact, the predictive uncertainty is commonly referred to as the 95% prediction uncertainty (95PPU). Two statistical indices can be used to quantify predictive uncertainty: (i) the p-factor, which measures the percentage of observed data falling within the 95PPU, and (ii) the r-factor, which is calculated as the ratio between the width of the 95PPU band and the standard deviation of the observed data. Ideally, the p-factor should range from 0.8 to 1.0, but in case of low-quality data, a value above 0.5 can be considered sufficient. The r-factor ranges from 0 to ∞, and ideally, its value should be <1. Achieving a balance between these two factors is crucial to ensure that most of the observed data fall within the 95PPU while minimizing the width of the uncertainty band.

3. Results

3.1. Assessment of models' performance based on optimal simulation

Table 4 presents the performance metrics for the best simulation in each scenario. As per Moriasi et al. (2007), the reference scenario S0 performed well in both the Tillouguite and Ait Ouchene sub-catchments, except for the validation in Ait Ouchene, where the NSE barely achieved 0.37 with a PBIAS of −37.06%. The evaluation of the single-variable models (S1-S8) in the two sub-catchments reveals stark differences in their performance. The Tillouguite sub-catchment presents a challenging scenario, as none of the models provided satisfactory results.

Table 4
Statistical criteria of the best simulation obtained from the last iteration.

Scenario	Nash Sutcliffe Efficiency (NSE)				Percent Bias (PBIAS)			
	Tillouguite		Ait Ouchene		Tillouguite		Ait Ouchene	
	Calibration	Validation	Calibration	Validation	Calibration	Validation	Calibration	Validation
S0:Q	0.63	0.58	0.82	0.38	-16.25	-27.65	-11.34	-37.06
S1:PML v2	-0.50	-1.08	0.77	0.41	-8.63	-19.62	13.62	-14.34
S2:TerraClimate	0.01	0.01	-0.71	-2.25	-12.84	-26.50	-75.33	-95.50
S3:FLDAS	0.31	0.42	0.73	0.19	36.07	22.25	-13.11	-37.26
S4:SSEBop	-1.14	-1.18	0.33	-0.47	-70.79	-78.19	-50.22	-70.78
S5:GLEAM v3.6a	0.16	0.11	0.74	0.41	-34.03	-44.02	-10.87	-30.64
S6:GLEAM v3.6b	0.25	0.23	0.73	0.19	3.82	-8.94	-13.11	-37.26
S7:MOD16A2	-2.23	-2.74	-3.19	-5.06	-82.20	-101.23	-156.19	-171.39
S8:GLDAS v2.1	0.35	0.34	0.15	-0.55	-14.84	-33.10	-63.22	-84.49
M1:Q & PML v2	0.63	0.58	0.81	0.40	-16.25	-27.65	1.51	-24.05
M2:Q & TerraClimate	0.61	0.55	0.73	0.38	-12.15	-23.65	4.20	-21.05
M3:Q & FLDAS	0.49	0.62	0.81	0.39	33.96	21.30	3.71	-24.05
M4:Q & SSEBop	0.63	0.58	0.82	0.38	-16.25	-27.65	-11.34	-37.06
M5:Q & GLEAM v3.6a	0.60	0.68	0.81	0.40	4.20	-5.50	1.51	-24.05
M6:Q & GLEAM v3.6b	0.60	0.68	0.81	0.40	4.20	-5.50	1.51	-24.05
M7:Q & MOD16A2	0.37	0.37	0.58	0.01	-45.57	-61.57	-39.63	-62.28
M8:Q & GLDAS v2.1	0.52	0.48	0.82	0.37	-27.46	-42.20	-11.34	-37.06
Legend	Minimum value of NSE			Maximum value of NSE	Maximum absolute value of PBIAS			Minimum absolute value of PBIAS

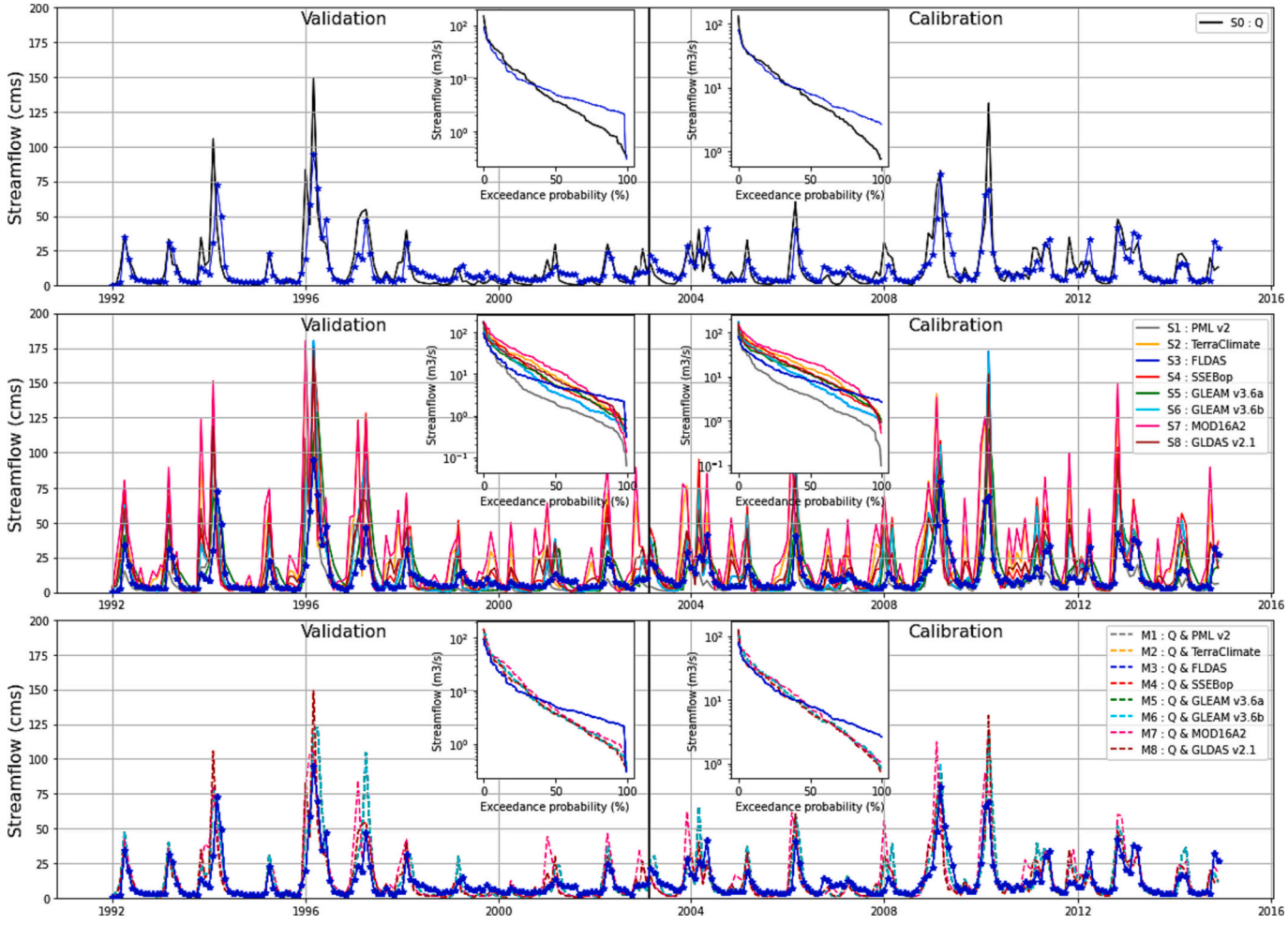

Fig. 3. Hydrographs of simulated vs observed discharge from the best parameter set according to each scenario (Tillouguite sub-catchment).

Nonetheless, the best-performing models in terms of NSE were GLDAS v2.1 (0.35), FLDAS (0.31), GLEAM v3.6b (0.25), and GLEAM v3.6a (0.16), in the given order. Meanwhile, the Ait Ouchene sub-catchment yielded encouraging results for some models, as PML v2, FLDAS, GLEAM v3.6a, and GLEAM v3.6b demonstrated outstanding performances, with NSE values exceeding 0.7 and PBIAS values below ±15%. On the other hand, MOD16A2 and SSEBop exhibited the poorest performance in terms of both NSE and PBIAS. Nevertheless, multi-variable models (M1-M8) outperform single-variable models (S1-S8) and the reference scenario (S0) in terms of NSE and PBIAS. When compared to S0, PBIAS was enhanced in most multi-variable models, and, more importantly, the streamflow validation was improved both in terms of NSE and PBIAS.

Fig. 3 and Fig. 4 present the hydrographs of the best simulation for each scenario in the Tillouguite and Ait Ouchene sub-catchments. The figures also illustrate the percentage of exceedance probability of both the observed and simulated values for each scenario during the calibration and validation phases. To better distinguish and visualize low values, the exceedance probability was plotted using a log10 normal probability scale. The visual analysis of the plot aligns with the statistical findings, providing further support to the results obtained. The reference scenario (S0) performed reasonably well, although it slightly overestimated peak values in years 1995/96 and 2009/10, particularly in the Tillouguite sub-catchment. On the other hand, single-variable models (S1-S8) had poor performance, resulting in higher peak estimates in both the Tillouguite and Ait Ouchene sub-catchments. The multi-variable models (M1-M8) performed significantly better in terms of peak values.

3.2. *Predictive uncertainty in streamflow simulations*

A further fundamental step consists in the analysis and quantification of the predictive uncertainty in streamflow simulations. Fig. 5 illustrates the results from the final iteration of the calibration and validation process, based on the two statistical criteria (r-factor and p-factor) mentioned in section 2.4. The r-factor and p-factor are projected onto a scatter plot, which enables a clear differentiation between the various investigated scenarios. into quantify. These two criteria represent a tool for the trade-off between the precision (via r-factor) and reliability (via p-factor) of model predictions across various calibration scenarios.

The calibration of the Tillouguite sub-catchment using the reference scenario (S0) resulted in a p-factor of 0.60 and a r-factor of 1.5. The single-variable models (S1-S8) exhibited a higher prediction uncertainty (higher r-factors) but captured a lesser portion of observed data (lower p-factors) compared to the baseline. Meanwhile, the multi-variable models M1, M2, M3, M5, and M6 had lower r-factors but higher p-factors compared to S0. In the validation, all scenarios had lower p-factors than S0, with the single-variable models showing a significant decrease compared with multi-variable models.

In the Ait Ouchene sub-catchment, the S0 model demonstrated the lowest p-factor in both calibration and validation. Single-variable models showed an increase in both r-factors and p-factors, suggesting a higher predictive uncertainty in their streamflow estimations. In contrast, certain multi-variable models reduced their r-factor when

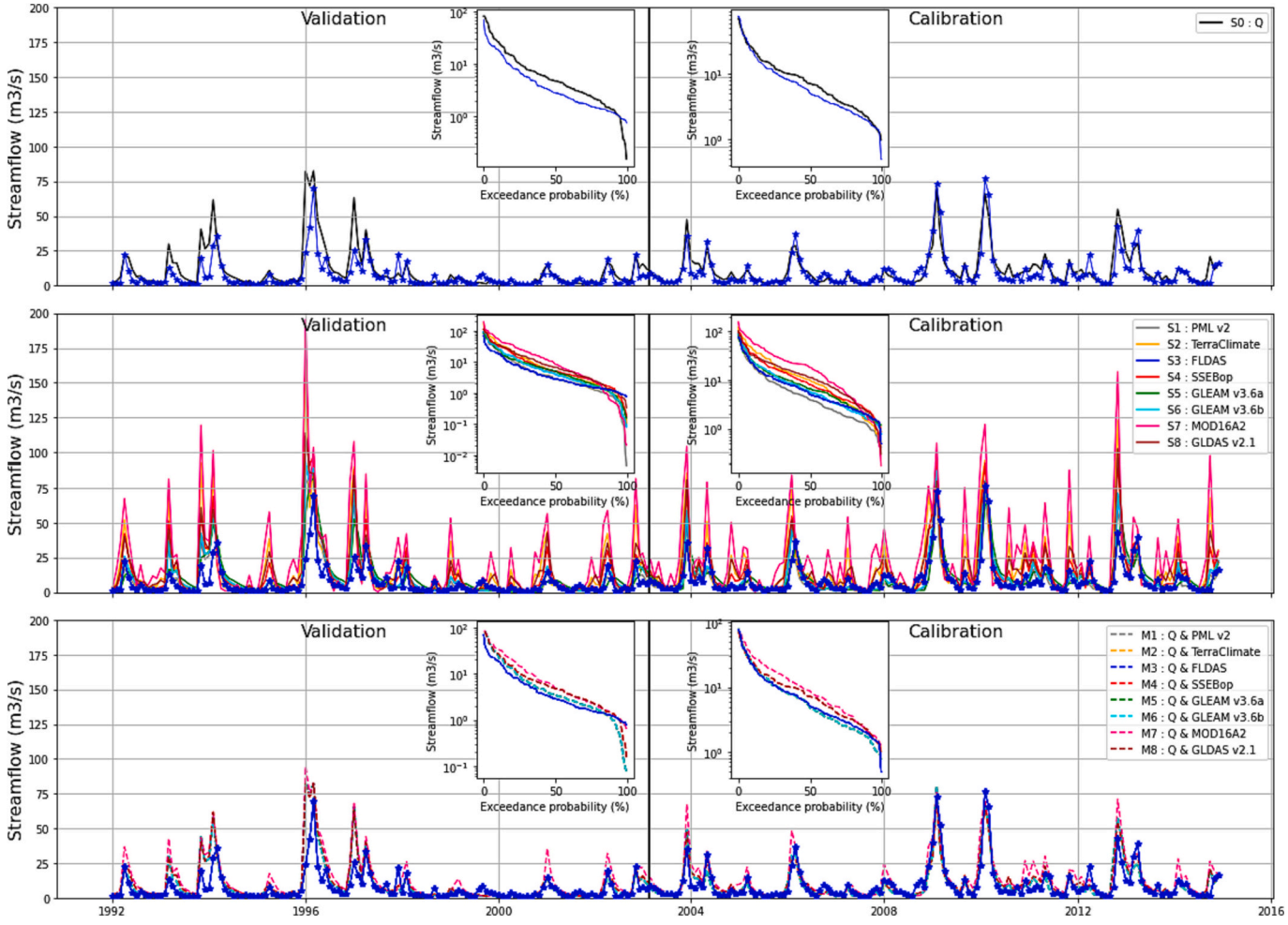

Fig. 4. Hydrographs of simulated vs observed discharge from the best parameter set according to each scenario (Ait Ouchene sub-catchment).

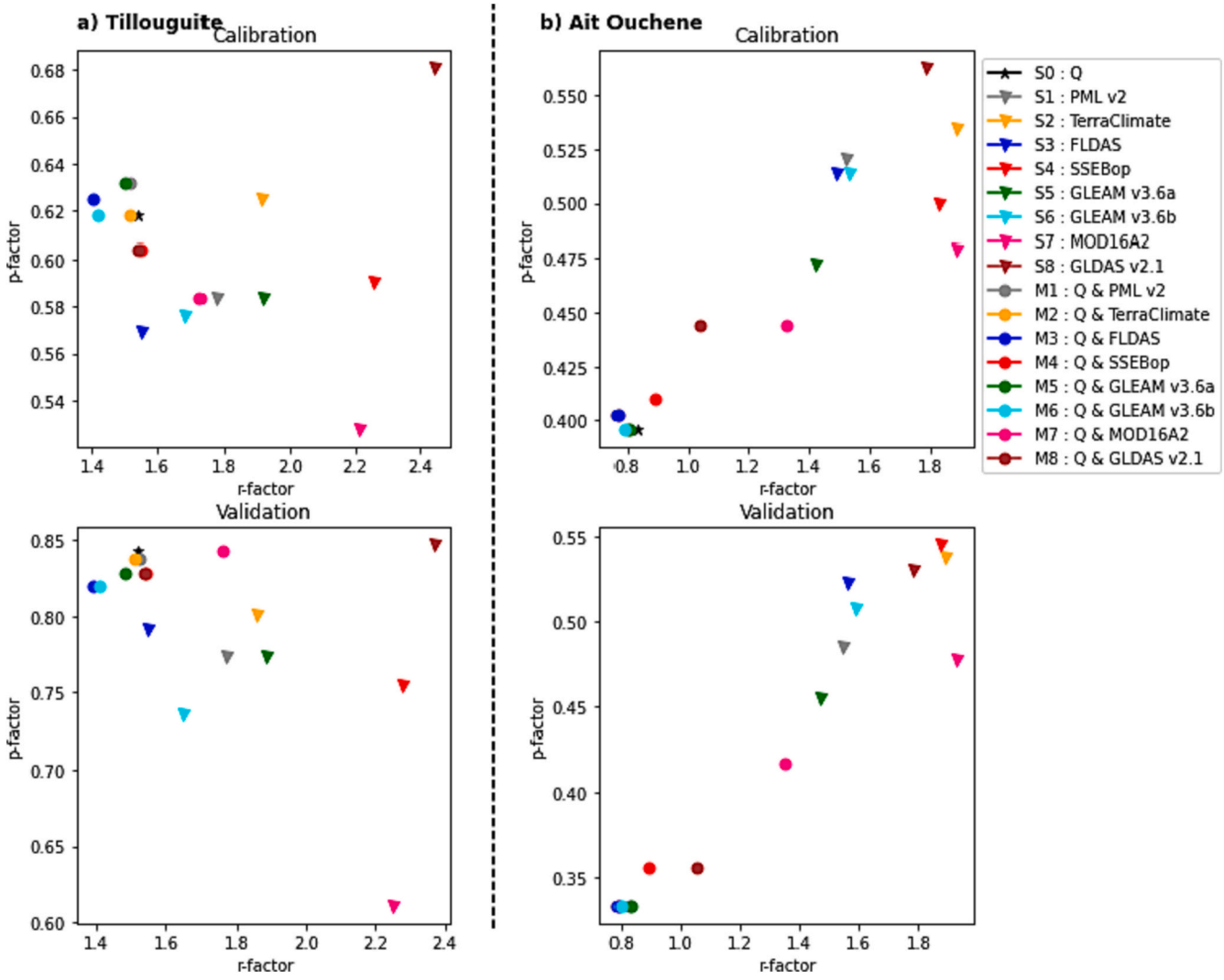

Fig. 5. 95PPU predictive uncertainty analysis of streamflow under different scenarios.

compared to the baseline scenario (S0), indicating a more precise prediction range.

3.3. Best-performing parameters' sets

3.3.1. Evaluation of parameters' uncertainties

To evaluate the uncertainty, posterior probability distributions were constructed from the top 100 performing parameter sets obtained from the final iterations of each scenario. These distributions were converted into a Gaussian density function (Houska et al., 2014). Every subplot displayed in Fig. 6 represents the distribution of one parameter according to each scenario. Due to the use of the Latin Hypercube sampling (Abbaspour et al., 2015), the prior distribution is a simple horizontal line. If no information is gained during the calibration period, the posterior distribution will be similar to the prior distribution (horizontal line), and the parameter will be regarded as unidentifiable. The more a parameter is identifiable, the more its posterior distribution will move from a horizontal line towards a single peak, implying less uncertainty about its optimal value (Houska et al., 2021).

According to the results, the S0 scenario displayed significant uncertainty when analysing the top 100 optimal parameter sets. This uncertainty is further emphasized by the observation of multiple peaks (multimodality) within the posterior parameter distributions. It is important to note that the incorporation of AET decreased the uncertainty for several parameters, including TLAPS, ESCO, SOL_BD, SLSOIL, and DLAI. This effect is particularly noticeable in the single-variable models (S1-S8), where the probability distributions for the aforementioned parameters exhibit a reduction in the posterior variance and a strong posterior distribution, implying lower degrees of uncertainty compared to S0. When examining the parameter distribution of the multi-variable models (M1 to M8), we found that for many parameters, the shape of the posterior distribution was somewhat similar to the S0 scenario. However, it's possible to observe some slight differences, which suggest a reduced range of posterior variance and a narrower posterior distribution.

It is noteworthy that using a particular dataset for the calibration of the SWAT model resulted in a diverse range of outcomes with regard to the parameter values. As an example, in the Tillouguite sub-catchment, the optimal TLAPS value was below −5 as per the results obtained from S5 and S7, whereas in the majority of cases, it ranged between 0 and − 5. This trend can be observed across multiple parameters, such as CANMX, CH_N2, CH_K2, ALPHA_BF, ESCO, and BLAI. However, the distribution of PLAPS was considerably narrowed by the majority of models, although the optimal values for all the models were relatively similar and close to 100 mm/km for both Tillouguite and Ait Ouchene sub-catchments. In fact, most of the models narrowed the posterior distribution of PLAPS to a similar optimal value for both sub-catchments. It can also be observed that the distribution of CN2 in the Ait Ouchene sub-catchment shows a similar trend.

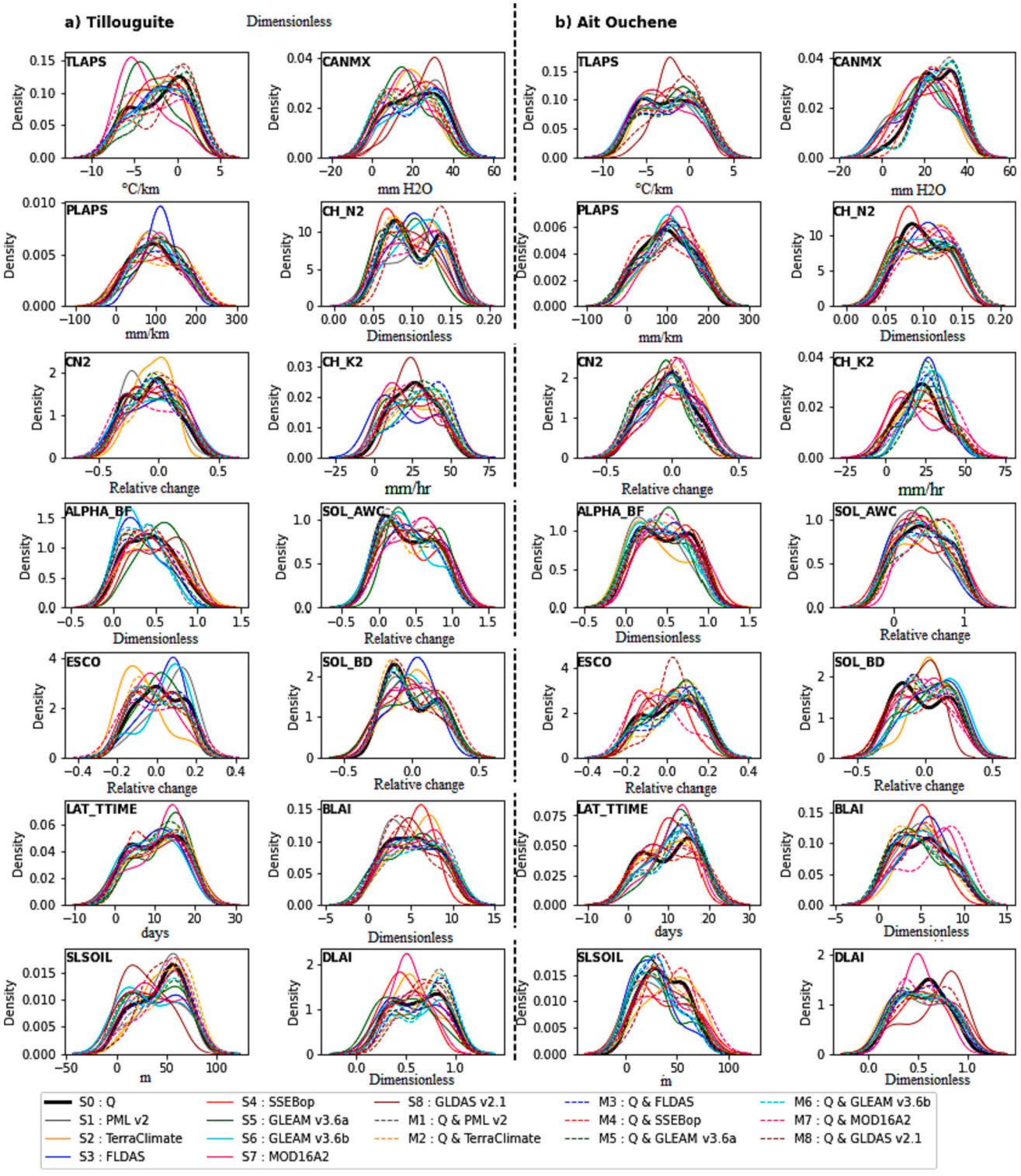

Fig. 6. Posterior distributions of 100 best-performing parameter sets in a) Tillouguite and b) Ait Ouchene.

3.3.2. *Equifinality in performance metrics*

Fig. 7 shows an evaluation of streamflow simulations obtained by using the top 100 performing parameter sets, in both the calibration and the validation phases. The box plots show the bounds of the performance metrics calculated. The first and second subplots illustrate the NSE and PBIAS metrics, respectively, obtained for the Tillouguite sub-catchment. The third and fourth subplots represent the same metrics for the Ait Ouchene sub-catchment. The red lines denote the thresholds regarded as satisfactory, as per Moriasi et al. (2007). In the S0 scenario, the median value of the boxplot indicated behavioural performance during the calibration for Ait Ouchene, whereas for Tillouguite it was <0.5. Furthermore, scenario S0 demonstrated the least variation in both NSE and PBIAS metrics as compared to other scenarios, and the performance spectrum of the best 100 simulations was the lowest. Conversely, the single-variable models (S1-S8) have larger variations and lower medians in terms of NSE values. When comparing different single-variable AET models, it was observed that scenario S3 exhibited the least amount of variation, while S7 and S8 showed the largest degree of variation.

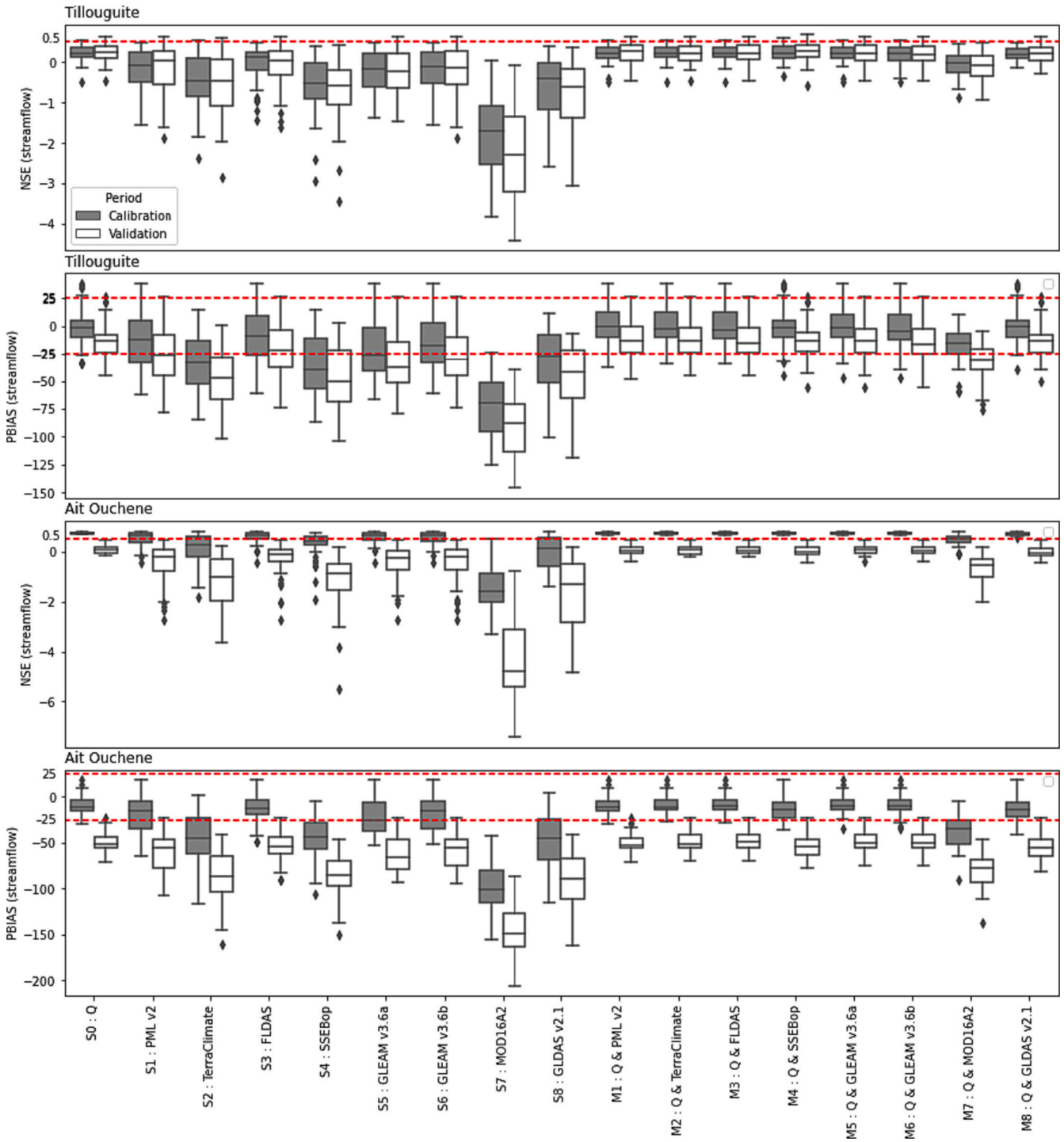

Fig. 7. Performance criteria (NSE and PBIAS) given by the 100 best-performing parameter sets in Tillouguite and Ait Ouchene.

Notably, S7 was unable to deliver satisfactory scores within its best-performing parameter sets. In multi-variable models (M1-M8), the boxes are smaller than those in single-variable models (S1-S8), but the variation is somewhat larger than that in the S0 model. With the exception of M7, the median values for most of the datasets used in multi-variable scenarios are closely clustered together.

3.3.3. *Uncertainties in water balance components*

Fig. 8 depicts the distribution of interannual averages for the water yield, AET, and soil moisture as simulated by SWAT, derived from the top 100 parameter sets, spanning the period between 1992 and 2015. When the SWAT model is calibrated using only the streamflow (S0), the top parameter sets exhibit a smaller variability in the simulated water yield, but a larger one in simulated AET and soil moisture, with respect to other models. On the other hand, when calibrating the SWAT model using only AET (S1-S8), the estimated AET and soil moisture exhibit less variabiity compared to the simulated water yield. The multi-variable models (M1-M8) showed relatively smaller variational bounds in the three simulated fluxes, including water yield, AET and soil moisture. Comparing the differences between the datasets used, it can be observed that calibrating with MOD16A2 and GLDAS v2.1 led to a relative overestimation of water yield, whereas AET and soil moisture were

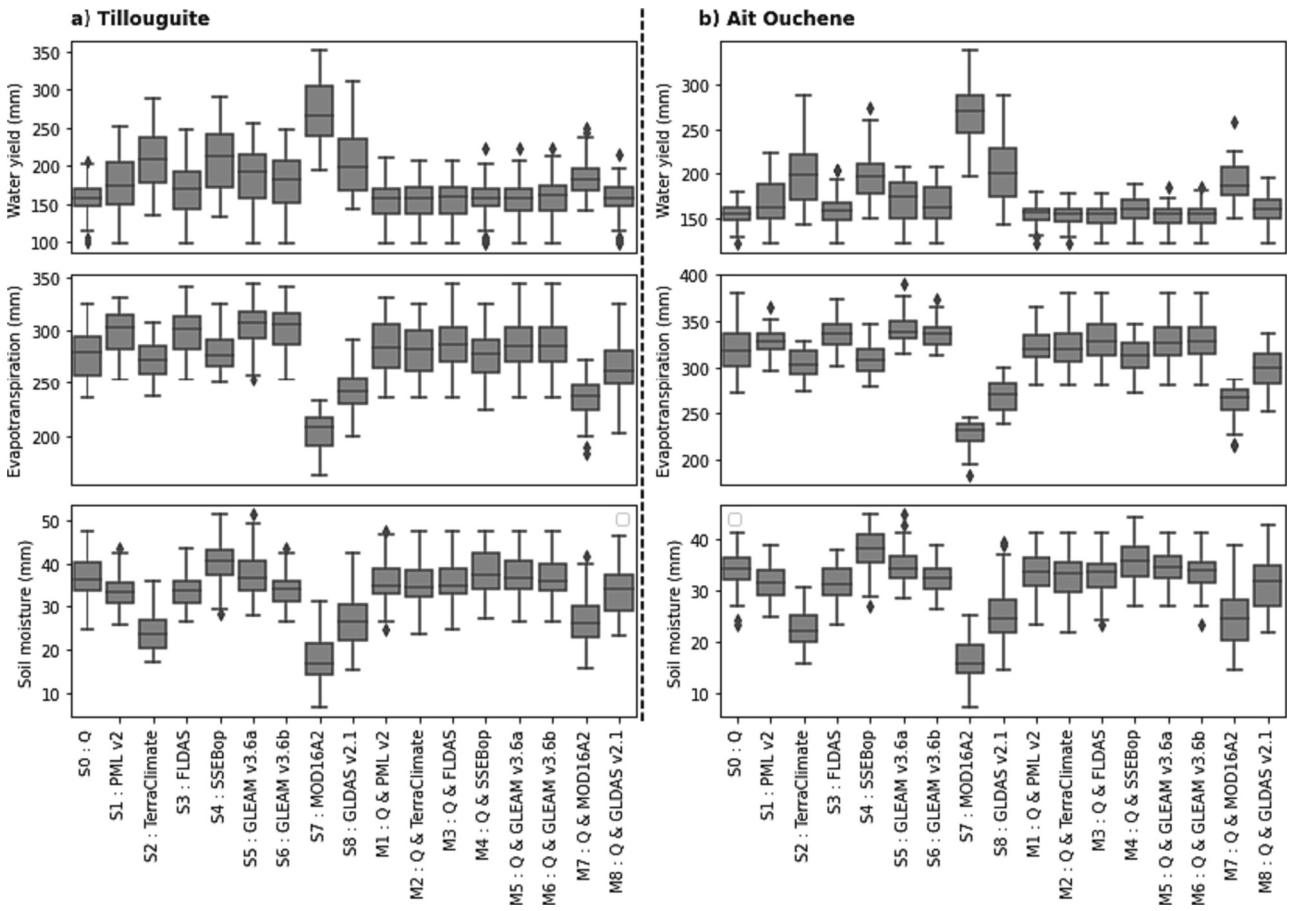

Fig. 8. Water balance components according to the 100 best-performing parameter sets under different scenarios: water yield, evapotranspiration, and soil moisture.

underestimated.

4. Discussion

4.1. Challenges and limitations of the streamflow-calibrated model

In the first scenario (S0), we used streamflow data from the outlets to calibrate the SWAT model, which is a common approach in the scientific community. In our case, this scenario serves as a benchmark for assessing the benefits of incorporating remotely sensed AET datasets. Despite S0 demonstrated a good level of agreement with the observed streamflow data (as shown in Table 4, Fig. 3 and Fig. 4), this scenario exhibited substantial uncertainty among the top 100 performing parameter sets, which is further underlined by the presence of multimodality in the posterior parameter distributions (Fig. 6). In fact, a posterior distribution that is highly multimodal reveals a scarce identification of the parameters. Additionally, most of these combinations of parameters generated comparable objective functions (as shown in Fig. 7) even if based on substantially different solutions, exemplifying an equifinality issue (Beven, 2006). This circumstance implies a non-uniqueness in the calibration process and the same streamflow observations can be replicated by different sets of parameters (Abbaspour et al., 2017), which could be explained by counter-balancing effects between parameters, structural uncertainty, or data limitations (Triana et al., 2019). The existence of compensating processes resulted in multiple parameter combinations that yield identical output signals. It is worth noting that distinct combinations represent underlying processes and assumptions about the system (Abbaspour et al., 2007), exacerbating the challenge of determining true parameter values by making the model predictions ambiguous. As shown in Fig. 8, when employing the top 100 performing parameter sets, S0 produced substantial variability in both AET and soil moisture, whereas it estimated a smaller variational range in the water yield.

Thus, the model's performance in forecasting streamflow does not necessarily imply the capability to accurately capture other hydrological variables, such as AET and soil moisture. Assuming that a particular model is sufficient to reproduce the hydrologic response of a system by considering solely its performance about the streamflow can be deceptive. Moreover, the equifinality may also stem from using a lumped calibration approach that simplifies the spatial representation of the hydrological system (Devia et al., 2015). It is conceivable that the point-calibrated model may not entirely capture the spatial complexities of the natural system, resulting in a greater degree of uncertainty in the distribution of the parameters. Another possible source of equifinality is the use of large parameter ranges, which might introduce ambiguity into the model's interpretations. Nevertheless, the findings of this paper align with other studies, suggesting that relying solely on streamflow data to calibrate a hydrological model may result in inadequate simulations of other variables, misleading downstream analysis such as drought, climate change impact, and environmental studies (Chen et al., 2023; Lee et al., 2022; Rajib et al., 2018; Sirisena et al., 2020; Wanders et al., 2014). Such inaccuracies can have significant implications for water management and policy decisions. Ultimately, it is critical for modelers to consider the limitations implied by the usage of streamflow data and the potential effects of equifinality when using them in calibrating hydrological models. To establish the validity of a hydrologic model, it must accurately depict the behaviour of all the system's variables.

4.2. Evaluating the efficacity of the AET-calibrated model in streamflow prediction

In order to demonstrate the effectiveness of AET products in predicting streamflow, we employed a single-variable approach to calibrate the SWAT model with the different global AET datasets (designated as S1 to S8). Unlike the streamflow-calibrated model (S0), which is represented by a single point, AET was incorporated spatially into each subbasin. Fig. 6 highlights a significant finding, i.e., AET integration narrowed down the posterior distributions of several key parameters, including PLAPS, ESCO, SOL_AWC, SOL_BD, SLSOIL, and DLAI, to a single optimum, enabling their identification. These parameters are related to soil moisture, water retention, transpiration, and leaf growth (Neitsch et al., 2011), which are all significant AET-influencing factors and their identification leads to a better streamflow prediction (Ferreira et al., 2021).

According to Table 4, the inclusion of AET data into the SWAT model's calibration for a single variable demonstrated mixed results in predicting streamflow. In the Ait Ouchene sub-catchment, a majority of single-variable AET models provided encouraging monthly streamflow estimates with NSE values surpassing 0.7 during the calibration phase. However, it's important to note that these models produced lower NSE values during the validation period, indicating some limitations in their predictive accuracy over different periods. For the Tillouguite sub-catchment, single-variable AET models were less effective, with the highest NSE value reached using GLDAS v2.1 at 0.35, trailed by FLDAS at 0.31, and GLEAM v3.6b at 0.25. Although single-variable AET models in some cases can provide reasonable streamflow estimates without direct streamflow measurements, the inconsistencies between calibration and validation periods, as well as between the two sub-catchments, are clearly showing the challenges of this approach. Additionally, while some single-variable AET calibrated models exhibited satisfactory performance (Table 4), other models presented suboptimal results, demonstrating a clear tendency towards overestimating peak flows by most of the single-variable AET models (Fig. 3 and Fig. 4), leading to significant negative PBIAS values, as shown in Table 4.

Moreover, the exceedance probability curves shown in the picture insets in Fig. 3 and Fig. 4 suggest that the calibration AET alone resulted in an increase of the probability of exceedance for high and median values, accompanied by a decrease in the probability of low flows. The graphical representation implies that most models provide better estimates of low flows compared to high and median values, which present larger discrepancies. Such a trend is particularly evident in the Ait Ouchene sub-catchment. According to Kunnath-Poovakka et al. (2016), and Odusanya et al. (2021), investigations into satellite-based AET calibration showed that catchments with high flows produce less precise forecasts compared to those with lower flows. This can be attributed to the rapid events that often characterise the high flows, which are not accounted for by the relatively slower process of AET, which in turn is based on satellite acquisitions that have a relatively slow revisit time. Differently from streamflow, AET appeared to be unsensitive to parameters such as ALPHA_BF, LAT_TIME, CH_K2, and CH_N2 (Fig. A1). The parameters' lack of sensitivity to AET may be attributed to either their negligible interaction with the process (Neitsch et al., 2011), or due to the inadequate range of values considered during the sensitivity analysis (Wu et al., 2022). These parameters are related to the routing of water through the stream network and the calculation of extreme values of streamflow. ALPHA_BF determines the proportion of baseflow in streamflow, while LAT_TIME affects the delay in the stream response to precipitation events. CH_K2 and CH_N2 determine the ease of water flow through the channel and the resistance to flow within the channel, respectively, which can impact the behaviour of the streamflow. Fig. 6 reveals a significant level of uncertainty in these parameters, which make them poorly constrained when using the AET alone. This implies that their values might have been scattered randomly across the best parameter sets produced by the single-variable AET models. By calibrating AET alone, the model may not be able to accurately estimate the optimal values for these parameters, leading to possible inaccurate predictions of the streamflow or other variables. Consequently, Fig. 8 suggests that using the top 100 performing parameter sets from calibrating AET alone leads to less variability in AET but larger variability in soil moisture and water yield.

Therefore, calibrating the model solely for AET without considering other water balance components may not sufficiently represent the entire water balance and can increase the uncertainty in soil moisture and streamflow. Similar studies suggested that, while the model performance may improve for the calibrated variable, it may decline for what regards the other variables (López López et al., 2017; Odusanya et al., 2021; Sirisena et al., 2020; Tobin and Bennett, 2020). Satisfactory streamflow performance is not always guaranteed by calibrating AET alone, and the good results obtained by some models could be attributed to the equifinality or the over-parametrisation of the parameters used, wherein distinct parameter sets can yield similar streamflow performances.

4.3. Improved predictability of the multi-variable calibration approach

For an optimal reproduction of the hydrological cycle, both vertical and horizontal flux components should be simultaneously constrained with relevant calibration targets. Therefore, a multi-variable approach was used to optimize the models based on AET and streamflow, with scenarios labelled M1 to M8. According to the results in Table 4, most of the multi-variable models obtained very good performances in terms of NSE values. However, during the calibration period, the NSE values for the eight multi-variable models frequently aligned with, or were even exceeded by, those of the S0 scenario. Fig. 3 and Fig. 4 also suggest similarities between the results for S0 and the multi-variable models. Ding and Zhu (2022) employed remote sensing-based AET to spatially calibrate the SWAT model and reported that their use of multi-variable calibration was also successful in validating the model. In our study, only three out of the eight multi-variable models showed better results than the S0 during the validation phase. This suggests that, while spatial AET products can have potential utility, their effectiveness might vary based on the specific context and conditions of the study.

From the exceedance probability curves illustrated in Fig. 3 and Fig. 4 (see the insets in each sub-plot), it can be inferred that the usage of multi-variable models led to significant enhancements in both high and median outcomes, resulting in considerable improvement in PBIAS values when compared to single calibration methods that rely solely on AET or streamflow. The improvement in PBIAS agrees with previous studies suggesting that, unless the horizontal and vertical fluxes are simultaneously adjusted, single calibrated models tend to underestimate or overestimate significantly the vertical water flux to the atmosphere (Odusanya et al., 2021; Rajib et al., 2018). Furthermore, multi-variable models reduced the uncertainties for several parameters (Fig. 6), as many parameters were easily identifiable, resulting in a reduced predictive uncertainty in streamflow compared to a single variable approach. This is because multi-variable models can better account for various parameters affecting multiple variables (Rajib et al., 2018; Rane and Jayaraj, 2022).

Our study found that the multi-variable models performed best, exhibiting a smaller variability of the water balance compared to the other models (Fig. 8), while also displaying better values in variability metrics than the baseline model S0 (Fig. 7). This suggests that the multi-variable models strike a good balance between reducing uncertainties in different simulated hydrological components and reducing equifinality in performance metrics.

It is worth noting that recent studies, such as those by Kunnath-Poovakka et al. (2021), and Wambura et al. (2018), suggested that using a multi-variable approach to constrain parameter sets can lead to fewer behavioural simulations.Jiang et al. (2020) used satellite-based AET for the spatially distributed calibration of the VIC model to determine the

effectiveness on simulated streamflow. They reported that the hydrologic model calibrated with AET can efficiently tune the relevant model parameters for better AET and streamflow simulations within their physically meaningful ranges. Similarly, Shah et al. (2021) hypothesized that the uncertainty problem associated with SWAT model could be improved by enhancing sub-processes embedded in the SWAT hydrological cycle, such as plant growth, AET, water yield, and soil–water balance, by applying remotely sensed AET data. Authors demonstrated the significance of this approach using a design experiment based on repeated measurements, in which the calibration was performed under both single variable and multi-variable schemes. Similar to our results, they showed that multi-variable calibration can improve the accuracy of streamflow simulation and reduce the equifinality of related parameters. Moreover, Dembélé et al. (2020) found that using evaporation data in addition to streamflow can enhance the model's proficiency in specific aspects, such as terrestrial water storage and soil moisture dynamics. Therefore, the use of multiple variables in calibrating the SWAT model can lead to improved predictability and a transition towards a better model state.

4.4. Comparing different AET products in hydrological modelling

The selection of the appropriate AET product is critical, due to differences in algorithms and approaches among these global datasets, as well as in their input data sources (Guo et al., 2022a). Thus, in order to evaluate how different products based on multiple sources affect the modelling of hydrological processes, we integrated eight freely accessible AET products into the SWAT model and compared their impact on model responses.

The findings of our study reveal that the inclusion of a specific dataset in the calibration of the SWAT model led to different results. In terms of sensitivity analysis, several parameters are commonly influencing AET scenarios. Nevertheless, the magnitude and ranking of sensitivity were different, depending on the AET data source used (Fig. A1). Furthermore, based on the Fig. 6, the shape of the posterior distribution for the top 100 performing parameter sets varies depending on which AET product is used. This suggests that the use of a specific dataset affects the model's output in a way that changes the parameter estimates. As a result, different datasets lead to different calibrated parameter sets, which consequently causes a different quantification of water resources in the region of study (Fig. 8). This happens because AET products may take different biases or uncertainties that affect the accuracy of the model's predictions. E.g., if one AET product consistently overestimates AET compared to the others, it provides different parameter values in the calibration of the SWAT model, which could have significant implications on the hydrological behaviour. Thus, modelers need to evaluate the performance of each product and carefully select the most appropriate AET product that delivers reasonable parameter estimates for a given case study.

GLEAM v3.6b and GLEAM v3.6a exhibited the best performance in our experiments, followed by FLDAS and PML v2 (as illustrated in Table 4). On the other hand, the capacity of MOD16A2, GLDAS v2.1, and SSEBop to calibrate the SWAT model was comparatively suboptimal. Notably, when MOD16A2 was employed in a single-variable calibration, the SWAT model displayed a remarkable negative PBIAS in streamflow, resulting in a dramatic overestimation of the peak values (Fig. 3 and Fig. 4). Even in a multi-variable calibration scheme, MOD16A2 performed the worst, resulting in larger negative PBIAS. The reason for this could be that MOD16A2 estimated the lowest amount of AET, compared to other AET products (as shown in Fig. 2). As a result, MOD16A2 decreases ESCO and TLAPS (Fig. 6), which ultimately leads to a reduction in the simulated AET. Consequently, MOD16A2 overestimated water yield while underestimated AET and soil moisture (Fig. 8). The decrease in AET to match MOD16A2 constrain is expected, nevertheless the model increased soil moisture simultaneously and increased in water yield. To our knowledge, no study has been carried out in the region using MOD16A2 product. However, recent studies investigated the performance of MOD16A2 in various regions and under different environmental conditions, and its ability to accurately estimate AET when used to calibrate hydrological models. Odusanya et al. (2019) calibrated the SWAT model with MOD16A2 product and found that it tended to underestimate AET. Jepsen et al. (2021) found that the dependence of MOD16A2 on vapor pressure deficit led to significant underestimations of AET during warm periods. Weerasinghe et al. (2020) used a water balance approach and found that MOD16A2 was less reliable compared to other AET products in Africa, particularly under water stress and drought conditions. Additionally, Huang et al. (2019), Ramoelo et al. (2014), and Tang et al. (2015) found low agreement between MOD16A2 and Eddy-Covariance flux data in South Africa, China, and Norway, respectively. Our results are in line with these studies suggesting that MOD16A2 may not be the most reliable AET product for certain regions and environmental conditions, and alternative AET products should be considered when calibrating the SWAT model. It is important to note that different studies, characterized by different conditions, yielded different results, even suggesting a better performance of MOD16A2 in calibrating hydrological models. For instance, Herman et al. (2020) found that SSEBop and MOD16A2 delivered the best streamflow and AET performance among eight AET datasets. In addition, Ding and Zhu (2022) indicated MOD16A2 as the best performing product in streamflow simulation when calibrating the SWAT model in a single-variable calibration.

However, GLDAS v2.1 and SSEBop, as well as TerraClimate, exhibited modest success, causing the model to unsatisfactory estimates of the streamflow, mainly in single variable calibration. The negative PBIAS in streamflow still occurs at low values, causing these models to slightly overestimate the streamflow peaks. In addition, TerraClimate, MOD16A2, SSEBop, and GLDAS v2.1 resulted in more uncertainty in streamflow predictions compared to other datasets (Fig. 5), while MOD16A2 was the weakest at bracketing measured streamflow inside the 95PPU. According to Table 4, GLEAM v3.6b and GLEAM v3.6a datasets performed the best among all the AET datasets in calibrating the SWAT model for streamflow. Previous studies confirmed the superiority of GLEAM data over other products in calibrating hydrological models. For example, Odusanya et al. (2019) used two AET products (GLEAM and MOD16A2) to calibrate the SWAT model for the data-sparse Ogun River Basin in southwestern Nigeria. They reported that the SWAT model using the Hargreaves PET equation and calibrated using the GLEAM_v3.0a data performed well for the simulation of AET and streamflow with acceptable predictive uncertainty. Furthermore, Ding and Zhu (2022) investigated the accuracy of multisource AET products and their applicability in hydrological modelling over a large catchment in China. They found that GLEAM has the lowest relative uncertainties, followed by MOD16A2 and GLDAS. Dembélé et al. (2020) analysed twelve sets of actual evaporation data to see if they could improve the performance of a distributed model. They tested four different multi-variable calibration strategies using both evaporation and streamflow data, and compared the results to a benchmark model calibrated only with streamflow data. The top three performing evaporation datasets were GLEAM v3.3a, SSEBop, and GLEAM v3.2a, while the bottom three were MOD16A2, CMRSET, and SEBS. According to the authors, the excellent performance of the GLEAM datasets was probably attributable to the Inclusion of soil moisture data in the computation of GLEAM AET (Martens et al., 2017). In a regional study, López López et al. (2017), used GLEAM data to calibrate the streamflow at Oum Er-Rbia. They reported good performance when using a step-wise calibration and a satisfactory streamflow prediction resulted from calibrating the model with AET alone.

4.5. Potentiality and limitations of this research

Although the present study provides valuable insights into the impact of incorporating remotely sensed AET products into a

hydrological model, this practice is subject to certain limitations that need to be analysed. Firstly, the investigation was conducted in two sub-catchments in the High Atlas region, and it is known that model performances are strongly depending on the peculiarities of the studied area, thus the rankings of the various experimented products are expected to be different. As an example, in this study several products of remote sensing-based AET achieved better performances in the single-variable calibration of Ait Ouchene compared to Tillouguite (Table 4). The performance of AET products can vary across regions, depending on a variety of factors including the specific location, climatic conditions, and the type of crop being grown locally (Guo et al., 2022a; Liaqat and Choi, 2017). Consequently, the global applicability of an AET product, i.e. its ability to be applied to other areas with different land cover types, weather patterns, and hydrological conditions may be limited.

This research emphasizes the potential of eight different satellite-based AET datasets to enhance streamflow, providing guidance for modelers to select the most suitable product for their specific applications. Additionally, this information can assist data developers in their efforts to enhance global estimations of AET (McCabe et al., 2019). However, it should be noted that the selection of these AET products was based on their accessibility and relevance to the study. It is possible that alternative products could have produced varying outcomes. Importantly, none of the AET products included in our investigation was compared to ground-based data inside the study region. Since the SWAT model is physically based, the fact that some products did better than others means that these products are more in line with the model conceptualization, but do not necessarily reflect the real accuracy. To better assess the accuracy of AET products, future studies should investigate adding Eddy-Covariance measurements. Furthermore, it is important to note that only AET datasets were employed to constrain the SWAT model. While AET is a crucial variable, using additional information such as soil moisture and LAI may have provided further insights (Rajib et al., 2020; Tobin and Bennett, 2020).

5. Conclusions

The main objectives of this study are: (1) to test the capacity of a single-variable calibration using eight freely available satellite-based AET products in the SWAT model for streamflow prediction, and (2) to examine the benefits of a dual-variable calibration (integrating remotely sensed AET and streamflow data) in enhancing the model's accuracy and parameter identification. Hence, we evaluated eight distinct AET datasets, including GLEAM v3.6a, GLEAM v3.6b, MOD16A2, GLDAS v2.1, PML v2, TerraClimate, FLDAS, and SSEBop, which were integrated into the calibration of the SWAT model. To optimize the parameterization and predictions by the model, we experimented with both a single and a multi-variable calibration approach, combining streamflow observations with the remotely-sensed AET. In summary, our investigation yielded the following key findings:

- Although the use of a streamflow-calibrated model (S0) generates a reasonable agreement with observed streamflow data, it can result in considerable uncertainty and equifinality in the calibration process. As a consequence, hydrological variables such as AET and soil moisture may not be adequately simulated, leading to potential impacts on water management and policy decisions. Though streamflow remains an indispensable data point in hydrological modelling, this observation emphasizes the need to complement it with other variables, especially when there are concerns about the model's comprehensiveness. Thus. it's essential to appreciate both the value and potential limitations of streamflow data in the calibration process.
- While some single-variable AET models provide satisfactory estimates of streamflow without relying on direct streamflow measurements, the calibration of AET alone may lead to overestimation of peak flows and increasing uncertainty in soil moisture and water yield. Thus, a calibration process relying solely on AET may take benefits, but caution should be exercised when using it.
- An approach based on the incorporation of multiple variables can significantly increase the precision of streamflow simulation compared to the single-variable approach mentioned above. By using AET and streamflow simultaneously, the models enhanced consistency and decreased variability, according to the performance metrics used. The application of AET products based on remote sensing contributed to a more stable streamflow simulation during the validation phase. Thus, this study highlights the potential taken by including multiple variables in the calibration of the hydrological cycle, in terms of improved predictability of the model.
- Different AET datasets led to different calibrated parameter sets, which consequently led to a different quantification of the hydrological cycle in the study area. GLEAM v3.6b and GLEAM v3.6a performed best among all AET datasets for calibrating the SWAT model as to streamflow, while MOD16A2 was the weakest in our study. Different AET products have different biases or uncertainties that affect the accuracy of the predictions, so modelers need to evaluate the performance of each product and carefully select the most appropriate for their specific case study.

At this end, the implications of our study extend beyond the Oued El Abid catchment and can be applied to other similar regions with at least similar climatic conditions, such as high variability in snow and evapotranspiration. By using the models that performed well in our study, hydrological modelers in similar areas can improve the accuracy of streamflow predictions, leading to better water management and allocation decisions. Also, assuming the importance of AET products for the calibration of overall hydrological models, the proposed approach can be used to individuate the most suitable AET product for a given area of interest, according to its peculiarities.

Accurate streamflow predictions can help the planning and operation of irrigation systems and the related reservoirs, as well as the assessment of water availability for all the possible stakeholders. Moreover, we highlighted the importance of selecting appropriate AET data for hydrological modelling, as different models perform differently in different regions. This emphasizes the need for further research to improve our understanding about the complex hydrological processes in different regions, and to develop more accurate AET products that can be used in hydrological modelling. These findings have practical implications in various sectors, including water resources management and hydrological forecasting. Therefore, this research aims to serve as a useful reference for future studies and practical applications in these fields, as a building block for the advancement of modelling capabilities.

Funding

This research did not receive any specific grant from funding agencies in the public, commercial, or not-for-profit sectors.

Data availability

The authors do not have permission to share data.

Appendix A. Results of the sensitivity analysis of parameters

The t-stat and *p*-value resulting from each combination of parameters and AET products is displayed in Fig. A1. This permits to identify which

parameters, for a given configuration of the model, will influence the simulation more. In general, the sensitivity of the parameters varies considerably between different scenarios. Except for CH_N2, and DLAI, the majority of parameters in a single-variable scenario (S0) have a *p-value* lower than 0.05, indicating a significant sensitivity to streamflow. While the sensitivity of BLAI to S0 was not significant in the Tillouguite sub-catchment, it was found to be considerably significant in the Ait Ouchene sub-catchment. Furthermore, the higher absolute values of t-stat obtained for PLAPS and CN2 in S0, followed by SOL_AWC, suggest that these parameters are the most sensitive to streamflow. However, several parameters including ALPHA_BF, LAT_TIME, CH_K2, and CH_N2, resulted poorly significant in single-variable AET scenarios (S1-S8). According to our metric, the sensitivity of the parameter CH_N2 can be considered insignificant (*p-value* > 0.05) in all the investigated scenarios. As depicted in Fig. A1, TLAPS, ESCO, SOL_AWC, and CANMX are more sensitive to the output when considering AET, either in single-variable calibration (S1 to S8) or in combination with streamflow in multi-variable calibration (M1 to M8). The inclusion of MOD16A2, in both scenarios S7 and M7, yielded a slightly higher negative value of t-stat for PLAPS, CANMX, and SOL_AWC compared to other datasets. While ESCO was not significantly sensitive to GLDAS v2.1 as a single-variable in both basins.

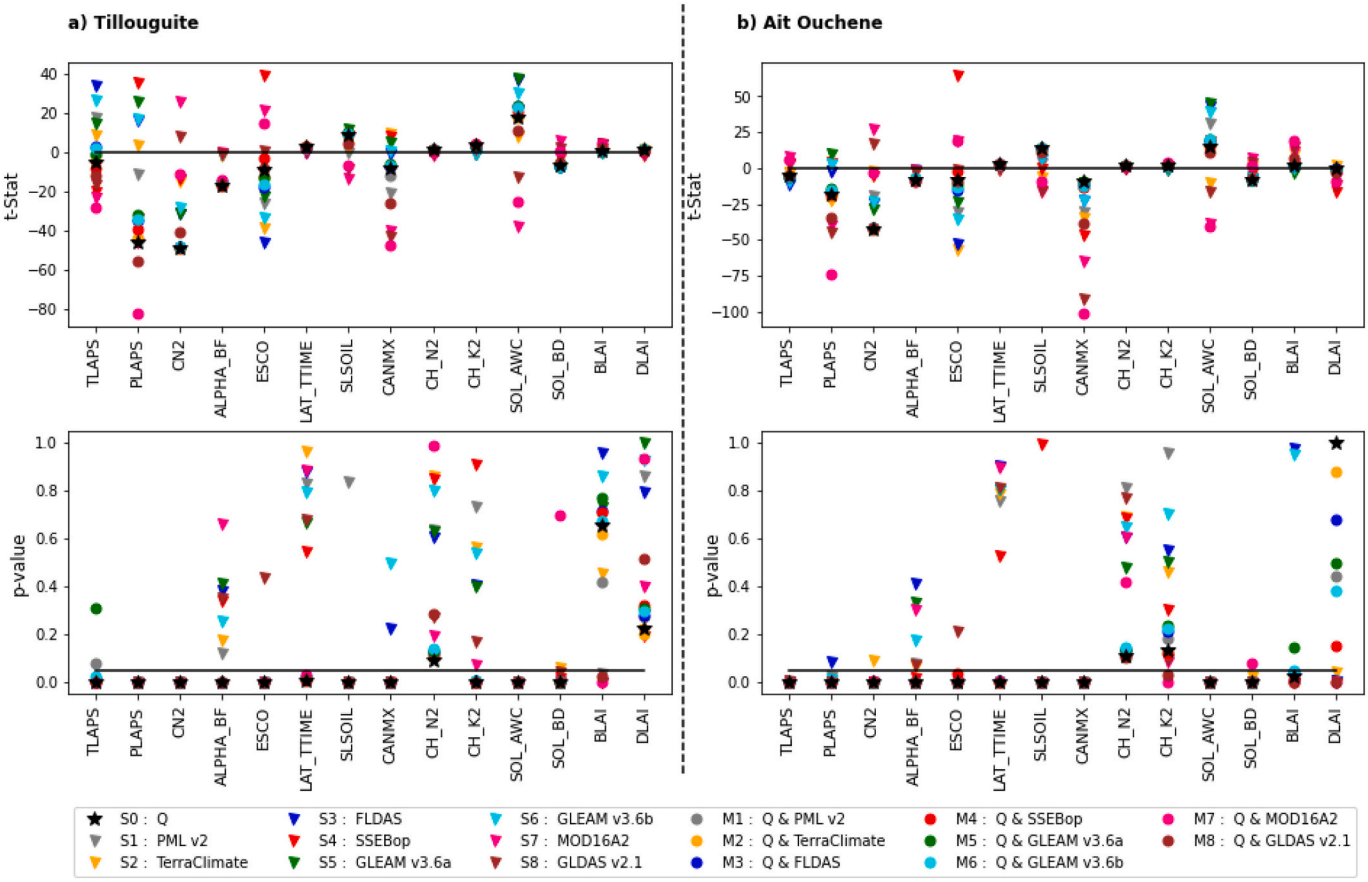

Fig. A1. Relative sensitivity analysis of the parameter under different scenarios.

References

Abatzoglou, J.T., Dobrowski, S.Z., Parks, S.A., Hegewisch, K.C., 2018. TerraClimate, a high-resolution global dataset of monthly climate and climatic water balance from 1958–2015. Sci Data 5, 1–12.

Abbaspour, K.C., 2013. Swat-cup 2012. SWAT calibration and uncertainty program—A user manual.

Abbaspour, K.C., Yang, J., Maximov, I., Siber, R., Bogner, K., Mieleitner, J., Zobrist, J., Srinivasan, R., 2007. Modelling hydrology and water quality in the pre-alpine/alpine Thur watershed using SWAT. J Hydrol (Amst) 333, 413–430.

Abbaspour, K.C., Rouholahnejad, E., Vaghefi, S., Srinivasan, R., Yang, H., Kløve, B., 2015. A continental-scale hydrology and water quality model for Europe: calibration and uncertainty of a high-resolution large-scale SWAT model. J Hydrol (Amst) 524, 733–752.

Abbaspour, K.C., Vaghefi, S.A., Srinivasan, R., 2017. A guideline for successful calibration and uncertainty analysis for soil and water assessment: a review of papers from the 2016 international SWAT conference. Water (Basel) 10, 6.

Acharki, S., Taia, S., Arjdal, Y., Hack, J., 2023. Hydrological modeling of spatial and temporal variations in streamflow due to multiple climate change scenarios in northwestern Morocco. Clim Serv 30, 100388.

Aryalekshmi, B.N., Biradar, R.C., Chandrasekar, K., Ahamed, J.M., 2021. Analysis of various surface energy balance models for evapotranspiration estimation using satellite data. Egypt. J. Remote Sens. Space Sci. 24, 1119–1126.

Beven, K., 2006. A manifesto for the equifinality thesis. J Hydrol (Amst) 320, 18–36.

Beven, K., Freer, J., 2001. Equifinality, data assimilation, and uncertainty estimation in mechanistic modelling of complex environmental systems using the GLUE methodology. J Hydrol (Amst) 249, 11–29.

Casado-Rodríguez, J., del Jesus, M., 2022. Hydrograph separation for tackling equifinality in conceptual hydrological models. J Hydrol (Amst) 610, 127816.

Chen, L., Wang, L., 2018. Recent advance in earth observation big data for hydrology. Big Earth Data 2, 86–107.

Chen, H., Gnanamoorthy, P., Chen, Y., Mansaray, L.R., Song, Q., Liao, K., Shi, A., Feng, G., Sun, C., 2022. Assessment and inter-comparison of multi-source high spatial resolution evapotranspiration products over Lancang–Mekong River Basin, Southeast Asia. Remote Sens. 14, 479.

Chen, S., Fu, Y.H., Wu, Z., Hao, F., Hao, Z., Guo, Y., Geng, X., Li, X., Zhang, X., Tang, J., 2023. Informing the SWAT model with remote sensing detected vegetation phenology for improved modeling of ecohydrological processes. J Hydrol (Amst) 616, 128817.

Dembélé, M., Ceperley, N., Zwart, S.J., Salvadore, E., Mariethoz, G., Schaefli, B., 2020. Potential of satellite and reanalysis evaporation datasets for hydrological modelling under various model calibration strategies. Adv. Water Resour. 143, 103667.

Devia, G.K., Ganasri, B.P., Dwarakish, G.S., 2015. A review on hydrological models. Aquat Procedia 4, 1001–1007.

Ding, J., Zhu, Q., 2022. The accuracy of multisource evapotranspiration products and their applicability in streamflow simulation over a large catchment of southern China. J Hydrol Reg Stud 41, 101092.

Efstratiadis, A., Koutsoyiannis, D., 2010. One decade of multi-objective calibration approaches in hydrological modelling: a review. Hydrol. Sci. J. – J. Des Sci. Hydrol. 55, 58–78.
El Khalki, E.M., Tramblay, Y., Hanich, L., Marchane, A., Boudhar, A., Hakkani, B., 2021. Climate change impacts on surface water resources in the Oued El Abid basin, Morocco. Hydrol. Sci. J. 66, 2132–2145.
Erraioui, L., Taia, S., Haida, S., Elmansouri, B., Chao, J., Mrabet, S., Taj-Eddine, K., 2020. Semi-distributed modeling of a large scale hydrological system using SWAT model. In: 2020 IEEE 2nd International Conference on Electronics, Control, Optimization and Computer Science, ICECOCS 2020. Institute of Electrical and Electronics Engineers Inc. https://doi.org/10.1109/ICECOCS50124.2020.9314540
Ferreira, R.G., Dias, R.L.S., de Siqueira Castro, J., dos Santos, V.J., Calijuri, M.L., da Silva, D.D., 2021. Performance of hydrological models in fluvial flow simulation. Ecol Inform 66, 101453.
Gleason, C.J., Durand, M.T., 2020. Remote sensing of river discharge: a review and a framing for the discipline. Remote Sens. 12, 1107.
Grusson, Y., Sun, X., Gascoin, S., Sauvage, S., Raghavan, S., Anctil, F., Sáchez-Pérez, J.-M., 2015. Assessing the capability of the SWAT model to simulate snow, snow melt and streamflow dynamics over an alpine watershed. J Hydrol (Amst) 531, 574–588.
Guo, Xiaotong, Meng, D., Chen, X., Li, X., 2022a. Validation and comparison of seven land surface evapotranspiration products in the Haihe River Basin, China. Remote Sens. 14, 4308.
Guo, Xiao, Wu, Z., He, H., Xu, Z., 2022b. Evaluating the potential of different evapotranspiration datasets for distributed hydrological model calibration. Remote Sens. 14, 629.
Gupta, A., Govindaraju, R.S., 2022. Uncertainty quantification in watershed hydrology: Which method to use? J Hydrol (Amst) 128749.
Hargreaves, G.H., Samani, Z.A., 1985. Reference crop evapotranspiration from temperature. Appl. Eng. Agric. 1, 96–99.
He, Z., Duethmann, D., Tian, F., 2021. A meta-analysis based review of quantifying the contributions of runoff components to streamflow in glacierized basins. J Hydrol (Amst) 603, 126890.
Her, Y., Seong, C., 2018. Responses of hydrological model equifinality, uncertainty, and performance to multi-objective parameter calibration. J. Hydroinf. 20, 864–885.
Herman, M.R., Nejadhashemi, A.P., Abouali, M., Hernandez-Suarez, J.S., Daneshvar, F., Zhang, Z., Anderson, M.C., Sadeghi, A.M., Hain, C.R., Sharifi, A., 2018. Evaluating the role of evapotranspiration remote sensing data in improving hydrological modeling predictability. J Hydrol (Amst) 556, 39–49.
Herman, M.R., Hernandez-Suarez, J.S., Nejadhashemi, A.P., Kropp, I., Sadeghi, A.M., 2020. Evaluation of multi-and many-objective optimization techniques to improve the performance of a hydrologic model using evapotranspiration remote-sensing data. J. Hydrol. Eng. 25, 04020006.
Houska, T., Multsch, S., Kraft, P., Frede, H.-G., Breuer, L., 2014. Monte Carlo-based calibration and uncertainty analysis of a coupled plant growth and hydrological model. Biogeosciences 11, 2069–2082.
Houska, T., Kraft, P., Jehn, F.U., Bestian, K., Kraus, D., Breuer, L., 2021. Detection of hidden model errors by combining single and multi-criteria calibration. Sci. Total Environ. 777, 146218.
Huang, S., Eisner, S., Magnusson, J.O., Lussana, C., Yang, X., Beldring, S., 2019. Improvements of the spatially distributed hydrological modelling using the HBV model at 1 km resolution for Norway. J Hydrol (Amst) 577, 123585.
Jepsen, S.M., Harmon, T.C., Guan, B., 2021. Analyzing the suitability of remotely sensed ET for calibrating a watershed model of a Mediterranean montane forest. Remote Sens. 13, 1258.
Jeyalakshmi, S., Chilkoti, V., Bolisetti, T., Balachandar, R., 2021. Earth data assimilation in hydrologic models: recent advances. Int. J. Environ. Stud. 78, 1003–1021.
Jiang, D., Wang, K., 2019. The role of satellite-based remote sensing in improving simulated streamflow: a review. Water (Basel) 11, 1615.
Jiang, L., Wu, H., Tao, J., Kimball, J.S., Alfieri, L., Chen, X., 2020. Satellite-based evapotranspiration in hydrological model calibration. Remote Sens. 12, 428.
Jin, X., Jin, Y., 2020. Calibration of a distributed hydrological model in a data-scarce basin based on GLEAM datasets. Water (Basel) 12, 897.
Kayastha, N., Lu, S., Betrie, G., Zakayo, Z., van Griensven, A., Solomatine, D., 2011. Dynamic linking of the watershed model SWAT to the multi-objective optimization tool NSGAX. In: Watermatex. 8th IWA Symposium on Systems Analysis and Integrated Assessment. IWA, San Sebastian, Spain, pp. 10–15.
Koltsida, E., Kallioras, A., 2022. Multi-variable SWAT model calibration using satellite-based evapotranspiration data and streamflow. Hydrology 9, 112.
Kunnath-Poovakka, A., Ryu, D., Renzullo, L.J., George, B., 2016. The efficacy of calibrating hydrologic model using remotely sensed evapotranspiration and soil moisture for streamflow prediction. J Hydrol (Amst) 535, 509–524.
Kunnath-Poovakka, A., Ryu, D., Eldho, T.I., George, B., 2021. Parameter uncertainty of a hydrologic model calibrated with remotely sensed evapotranspiration and soil moisture. J. Hydrol. Eng. 26, 04020070.
Lee, S., Qi, J., McCarty, G.W., Anderson, M., Yang, Y., Zhang, X., Moglen, G.E., Kwak, D., Kim, H., Lakshmi, V., 2022. Combined use of crop yield statistics and remotely sensed products for enhanced simulations of evapotranspiration within an agricultural watershed. Agric. Water Manag. 264, 107503.
Liaqat, U.W., Choi, M., 2017. Accuracy comparison of remotely sensed evapotranspiration products and their associated water stress footprints under different land cover types in Korean peninsula. J. Clean. Prod. 155, 93–104.
Liu, Z., Yin, J., Dahlke, E.H., 2020. Enhancing soil and water assessment tool snow prediction reliability with remote-sensing-based snow water equivalent reconstruction product for upland watersheds in a multi-objective calibration process. Water (Basel) 12, 3190.
López López, P., Sutanudjaja, E.H., Schellekens, J., Sterk, G., Bierkens, M.F.P., 2017. Calibration of a large-scale hydrological model using satellite-based soil moisture and evapotranspiration products. Hydrol. Earth Syst. Sci. 21, 3125–3144.
Martens, B., Miralles, D.G., Lievens, H., Van Der Schalie, R., De Jeu, R.A.M., Fernández-Prieto, D., Beck, H.E., Dorigo, W.A., Verhoest, N.E.C., 2017. GLEAM v3: satellite-based land evaporation and root-zone soil moisture. Geosci. Model Dev. 10, 1903–1925.
McCabe, M.F., Miralles, D.G., Holmes, T.R.H., Fisher, J.B., 2019. Advances in the remote sensing of terrestrial evaporation. Remote Sens. 11, 1138.
McNally, A., Arsenault, K., Kumar, S., Shukla, S., Peterson, P., Wang, S., Funk, C., Peters-Lidard, C.D., Verdin, J.P., 2017. A land data assimilation system for sub-Saharan Africa food and water security applications. Sci Data 4, 1–19.
Moges, E., Demissie, Y., Larsen, L., Yassin, F., 2021. Sources of hydrological model uncertainties and advances in their analysis. Water (Basel) 13, 28.
Monteith, J.L., 1965. Evaporation and environment. In: Symposia of the Society for Experimental Biology. Cambridge University Press (CUP), Cambridge, pp. 205–234.
Moriasi, D.N., Arnold, J.G., Van Liew, M.W., Bingner, R.L., Harmel, R.D., Veith, T.L., 2007. Model evaluation guidelines for systematic quantification of accuracy in watershed simulations. Trans. ASABE 50, 885–900.
Mu, Q., Heinsch, F.A., Zhao, M., Running, S.W., 2007. Development of a global evapotranspiration algorithm based on MODIS and global meteorology data. Remote Sens. Environ. 111, 519–536.
Mu, Q., Zhao, M., Running, S.W., 2011. Improvements to a MODIS global terrestrial evapotranspiration algorithm. Remote Sens. Environ. 115, 1781–1800.
Neitsch, S.L., Arnold, J.G., Kiniry, J.R., Williams, J.R., 2011. Soil and Water Assessment Tool Theoretical Documentation Version 2009. Texas Water Resources Institute.
Nourani, V., Tootoonchi, R., Andaryani, S., 2021. Investigation of climate, land cover and lake level pattern changes and interactions using remotely sensed data and wavelet analysis. Ecol Inform 64, 101330.
Odusanya, A.E., Mehdi, B., Schürz, C., Oke, A.O., Awokola, O.S., Awomeso, J.A., Adejuwon, J.O., Schulz, K., 2019. Multi-site calibration and validation of SWAT with satellite-based evapotranspiration in a data-sparse catchment in southwestern Nigeria. Hydrol. Earth Syst. Sci. 23, 1113–1144.
Odusanya, A.E., Schulz, K., Biao, E.I., Degan, B.A.S., Mehdi-Schulz, B., 2021. Evaluating the performance of streamflow simulated by an eco-hydrological model calibrated and validated with global land surface actual evapotranspiration from remote sensing at a catchment scale in West Africa. J Hydrol Reg Stud 37, 100893.
Priestley, C.H.B., Taylor, R.J., 1972. On the assessment of surface heat flux and evaporation using large-scale parameters. Mon. Weather Rev. 100, 81–92.
Rahman, K., Maringanti, C., Beniston, M., Widmer, F., Abbaspour, K., Lehmann, A., 2013. Streamflow modeling in a highly managed mountainous glacier watershed using SWAT: the Upper Rhone River watershed case in Switzerland. Water Resour. Manag. 27, 323–339.
Rajib, A., Evenson, G.R., Golden, H.E., Lane, C.R., 2018. Hydrologic model predictability improves with spatially explicit calibration using remotely sensed evapotranspiration and biophysical parameters. J Hydrol (Amst). https://doi.org/10.1016/j.jhydrol.2018.10.024.
Rajib, A., Kim, I.L., Golden, H.E., Lane, C.R., Kumar, S.V., Yu, Z., Jeyalakshmi, S., 2020. Watershed modeling with remotely sensed big data: MODIS leaf area index improves hydrology and water quality predictions. Remote Sens. 12, 2148.
Ramoelo, A., Majozi, N., Mathieu, R., Jovanovic, N., Nickless, A., Dzikiti, S., 2014. Validation of global evapotranspiration product (MOD16) using flux tower data in the African savanna, South Africa. Remote Sens. 6, 7406–7423.
Rane, N.L., Jayaraj, G.K., 2022. Enhancing SWAT model predictivity using multi-objective calibration: effects of integrating remotely sensed evapotranspiration and leaf area index. Int. J. Environ. Sci. Technol. 1–20.
Rodell, M., Houser, P.R., Jambor, U.E.A., Gottschalck, J., Mitchell, K., Meng, C.-J., Arsenault, K., Cosgrove, B., Radakovich, J., Bosilovich, M., 2004. The global land data assimilation system. Bull. Am. Meteorol. Soc. 85, 381–394.
Salazar-Martínez, D., Holwerda, F., Holmes, T.R.H., Yépez, E.A., Hain, C.R., Alvarado-Barrientos, S., Ángeles-Pérez, G., Arredondo-Moreno, T., Delgado-Balbuena, J., Figueroa-Espinoza, B., 2022. Evaluation of remote sensing-based evapotranspiration products at low-latitude eddy covariance sites. J Hydrol (Amst) 610, 127786.
Schlesinger, W.H., Jasechko, S., 2014. Transpiration in the global water cycle. Agric. For. Meteorol. 189, 115–117.
Senay, G.B., Bohms, S., Singh, R.K., Gowda, P.H., Velpuri, N.M., Alemu, H., Verdin, J.P., 2013. Operational evapotranspiration mapping using remote sensing and weather datasets: a new parameterization for the SSEB approach. JAWRA J. Am. Water Resourc. Assoc. 49, 577–591.
Shah, S., Duan, Z., Song, X., Li, R., Mao, H., Liu, J., Ma, T., Wang, M., 2021. Evaluating the added value of multi-variable calibration of SWAT with remotely sensed evapotranspiration data for improving hydrological modeling. J Hydrol (Amst) 603, 127046.
Shawky, M., Ahmed, M.R., Ghaderpour, E., Gupta, A., Achari, G., Dewan, A., Hassan, Q. K., 2023. Remote sensing-derived land surface temperature trends over South Asia. Ecol Inform 74, 101969.
Sirisena, T.A.J.G., Maskey, S., Ranasinghe, R., 2020. Hydrological model calibration with streamflow and remote sensing based evapotranspiration data in a data poor basin. Remote Sens. 12, 3768.
Strauch, M., Bernhofer, C., Koide, S., Volk, M., Lorz, C., Makeschin, F., 2012. Using precipitation data ensemble for uncertainty analysis in SWAT streamflow simulation. J Hydrol (Amst) 414, 413–424.
Sun, P., Wu, Y., Xiao, J., Hui, J., Hu, J., Zhao, F., Qiu, L., Liu, S., 2019. Remote sensing and modeling fusion for investigating the ecosystem water-carbon coupling processes. Sci. Total Environ. 697, 134064.

Taia, S., Erraioui, L., Mbrenga, N.C., Chao, J., El Mansouri, B., Haida, S., Taj-Eddine, K., 2021. Assessment of soil erosion using two spatial approaches: RUSLE and SWAT Model. In: E3S Web of Conferences. EDP Sciences, p. 82.

Taia, S., Erraioui, L., Arjdal, Y., Chao, J., El Mansouri, B., Scozzari, A., 2023. The application of SWAT model and remotely sensed products to characterize the dynamic of streamflow and snow in a mountainous watershed in the high atlas. Sensors 23, 1246.

Tang, R., Shao, K., Li, Z.-L., Wu, H., Tang, B.-H., Zhou, G., Zhang, L., 2015. Multiscale validation of the 8-day MOD16 evapotranspiration product using flux data collected in China. IEEE J Sel Top Appl Earth Obs Remote Sens 8, 1478–1486.

Tobin, K.J., Bennett, M.E., 2020. Improving SWAT model calibration using soil MERGE (SMERGE). Water (Basel) 12, 2039.

Triana, J.S.A., Chu, M.L., Guzman, J.A., Moriasi, D.N., Steiner, J.L., 2019. Beyond model metrics: the perils of calibrating hydrologic models. J Hydrol (Amst) 578, 124032.

Tuel, A., Chehbouni, A., Eltahir, E.A.B., 2021. Dynamics of seasonal snowpack over the high atlas. J Hydrol (Amst) 595, 125657. https://doi.org/10.1016/j.jhydrol.2020.125657.

Ukkola, A.M., Prentice, I.C., 2013. A worldwide analysis of trends in water-balance evapotranspiration. Hydrol. Earth Syst. Sci. 17, 4177–4187.

Ustin, S.L., Middleton, E.M., 2021. Current and near-term advances in Earth observation for ecological applications. Ecol. Process. 10, 1–57.

Van Buuren, S., Groothuis-Oudshoorn, K., 2011. Mice: multivariate imputation by chained equations in R. J. Stat. Softw. 45, 1–67.

Wambura, F.J., Dietrich, O., Lischeid, G., 2018. Improving a distributed hydrological model using evapotranspiration-related boundary conditions as additional constraints in a data-scarce river basin. Hydrol. Process. 32, 759–775.

Wanders, N., Bierkens, M.F.P., de Jong, S.M., de Roo, A., Karssenberg, D., 2014. The benefits of using remotely sensed soil moisture in parameter identification of large-scale hydrological models. Water Resour. Res. 50, 6874–6891.

Weerasinghe, I., Bastiaanssen, W., Mul, M., Jia, L., Van Griensven, A., 2020. Can we trust remote sensing evapotranspiration products over Africa? Hydrol. Earth Syst. Sci. 24, 1565–1586.

Wu, L., Liu, X., Chen, J., Yu, Y., Ma, X., 2022. Overcoming equifinality: time-varying analysis of sensitivity and identifiability of SWAT runoff and sediment parameters in an arid and semiarid watershed. Environ. Sci. Pollut. Res. 29, 31631–31645.

Zhang, K., Kimball, J.S., Running, S.W., 2016. A review of remote sensing based actual evapotranspiration estimation. Wiley Interdiscip. Rev. Water 3, 834–853.

Zhang, Y., Kong, D., Gan, R., Chiew, F.H.S., McVicar, T.R., Zhang, Q., Yang, Y., 2019. Coupled estimation of 500 m and 8-day resolution global evapotranspiration and gross primary production in 2002–2017. Remote Sens. Environ. 222, 165–182.